WPEDU-PR(18) 21446

S Nasr et al.

Gyro-kinetic theory and global simulations of the collisionless tearing instability: the impact of trapped particles through the magnetic field curvature

Preprint of Paper to be submitted for publication in
Physics of Plasmas

This work has been carried out within the framework of the EUROfusion Consortium and has received funding from the Euratom research and training programme 2014-2018 under grant agreement No 633053. The views and opinions expressed herein do not necessarily reflect those of the European Commission.

Gyro-kinetic theory and global simulations of the collisionless tearing instability: the impact of trapped particles through the magnetic field curvature

S. Nasr,[1] D. Zarzoso,[1] X. Garbet,[2] A. I. Smolyakov,[3] W. A. Hornsby,[4] and S. Benkadda[1]
[1)] *Aix-Marseille Université, CNRS PIIM, UMR 7345 Marseille, France*
[2)] *CEA, IRFM, F-13108 St. Paul-lez-Durance Cedex, France*
[3)] *Department of Physics and Engineering Physics, University of Saskatchewan, Saskatoon, Canada*
[4)] *Theoretical Physics V, Department of Physics, Universitaet Bayreuth, Bayreuth D-95447, Germany*

The linear instability of the tearing mode is analysed using a gyro-kinetic approach within a Hamiltonian formalism, where the interaction between particles and the tearing mode through the wave-particle resonance is retained. It is shown that the presence of trapped particles leads to an overall increase of the growth rate of the tearing instability. In addition, the curvature of the magnetic field is shown to play no role in the linear instability when only passing particles are present in the plasma. Gyro-kinetic simulations using the state-of-the-art Gkw code confirm these findings and are further used to evidence the impact of the magnetic field curvature and the temperature gradient in the presence of a population of trapped particles. It is observed numerically that the curvature modifies the stability of the tearing mode by means of trapped particles. Two cases are reported. First, without any temperature gradient, it tends to stabilize the tearing mode through wave-particle resonance with the trapped electrons. Second, with increasing temperature gradient, magnetic curvature tends to destabilize the mode, suggesting an interchange mechanism. The balance of these two stabilizing/destabilizing effects leads to a threshold in temperature gradient beyond which the magnetic curvature plays a destabilizng role. This opens the way to a deeper understading and control of the tearing instability in fusion plasmas.

I. INTRODUCTION: THE GYROKINETIC MODEL TO DESCRIBE THE TEARING INSTABILITY

In magnetised laboratory and space plasmas, a special class of instabilities can occur in the presence of non-ideal effects (such as resistivity or inertia) and can tear apart the magnetic field lines resulting in their reconnection. This process leads to a modification of the magnetic topology, characterised by the formation of magnetic islands. For this reason, these instabilities are called tearing instabilities. Their understanding is of prime importance in plasmas, since they increase the transport of particles, degrading the confinement and eventually leading to disruptions in laboratory plasmas.

The tearing mode instability has been extensively studied in the framework of MagnetoHydroDynamics (MHD) theory. The main assumption has been high dissipation in the form of collisional resistivity. However future tokamaks are expected to operate at very low collisionality, thus the need to treat this instability in the collisionless limit. In addition, particles in a tokamak exhibit different types of trajectories, characterised by different frequencies and scales. So far, the kinetic aspects of the tearing instability steming from the trajectories and the resonances between particles and the tearing mode has not been analysed in detail. For this purpose, a self-consistent and more accurate calculation is required. One needs in particular to consider a kinetic modeling of the plasma, where the kinetic effects are intrinsically included. Of course, a fully kinetic model is extremely complicated due to the high dimensionality of the problem. For this reason, we will make use of the gyro-kinetic approach, consisting upon averaging over the gyromotion of the particle to reduce the dimensionality. In this paper we will therefore present a gyro-kinetic description of the tearing mode and we will analyse the impact of trapped particles on its linear excitation. This will be done with analytic theory and with global gyro-kinetic simulations, through which we will also perform an extensive parametric study of the tearing instability. The remainder of the paper is structured as follows. In section II, we derive, within the gyro-kinetic approach, the perturbed parallel current using a Hamiltonian formalism. Section III is devoted to the derivation of the tearing mode dispersion relation. This will be done by integration of Ampère's law, under the so-called constant-ψ approximation and separating the radial domain into an ideal MHD (outer) region where kinetic effects are negligible and where we calculate numerically the so-called tearing stability parameter (Δ'), and a non-ideal (inner) region where kinetic effects are retained through the wave-particle resonance. In section IV the different resonances between the tearing mode and the particles are studied analytically and the presence of trapped particles is shown to increase the growth rate of the instability. We also show that the magnetic curvature does not play any role in the tearing instability when only passing particles are considered. Section V is devoted to the numerical analysis using Gkw simulations. We will in particular confirm the analytic results and study in detail the impact of trapped particles, curvature and temperature gradient. In section VI we report on the different responses of particles to the tearing instability through an energy exchange diagnostic. We evidence in particular the interaction between trapped particles and the tearing mode.

II. HAMILTONIAN FORMALISM TO CALCULATE THE PERTURBED PARALLEL CURRENT WITHIN A GYRO-KINETIC APPROACH

The tearing instability can be described at the simplest level using Ampère's law

$$\nabla \times (\nabla \times \mathbf{A}) = \mu_0 \mathbf{j} \tag{1}$$

where $\mathbf{A}$ is the vector potential, $\mathbf{j}$ is the current and μ_0 is the vacuum permeability. We assume that we have only parallel component of $\mathbf{A}$. Therefore $\mathbf{A} = \delta A_\parallel \mathbf{b}$, where $\mathbf{b}$ is the unit vector along the magnetic field lines. Projecting onto the parallel direction straightforwardly gives an equation for the perturbed parallel current $j_\parallel$

$$\nabla_\perp^2 \delta A_\parallel = -\mu_0 j_\parallel \tag{2}$$

that has to be integrated to obtain the dispersion relation. In Eq.(2), $\nabla_\perp^2$ is the Laplacian operator in the direction perpendicular to the equilibrium magnetic field.

In the following, we assume that the main response is that of electrons. Therefore, in order to calculate the perturbed parallel current, we will first of all calculate the exact linear response of electrons, which will yield the perturbed parallel current after integration in velocity space. The details of this calculation are given in Appendix A. The idea is to start with the Vlasov equation in conservative form using a Hamiltonian formalism

$$\frac{\partial F}{\partial t} - [\mathcal{H}, F] = 0 \tag{3}$$

where $[X, Y]$ represents the Poisson brackets between X and Y, i.e. $[X, Y] = \partial_{\mathbf{x}} X \partial_{\mathbf{p}} Y - \partial_{\mathbf{p}} X \partial_{\mathbf{x}} Y$, where $\mathbf{x}$ and $\mathbf{p}$ are the position and momenta, forming a set of canonical variables satisfying Hamilton's equations. We can introduce another system of canonically conjugated variables, satisfying Hamilton's equations, especially suitable for the analysis of particles in a tokamak, since they reflect the three directions of periodicity of the trajectories. These are the angle-action variables $\boldsymbol{\alpha}, \mathbf{J}$, with $\boldsymbol{\alpha} = (\alpha_1, \alpha_2, \alpha_3)$ and $\mathbf{J} = (J_1, J_2, J_3)$, where α_1 represents the gyro-phase, α_2 represents the periodicity angle in the poloidal direction and α_3 represents the periodicity angle in the toroidal direction. The actions are motion invariants associated to each direction of the particle trajectory. In particular, J_1 is proportional to the magnetic moment $\mu = m_e v_\perp / (2B)$ and J_3 is the toroidal canonical momentum $J_3 \equiv P_\varphi = -eZ_e\psi + m_e R v_\varphi$, with m_e the electron mass, $v_\perp$ the projection of the electron velocity onto the direction perpendicular to the magnetic field, B is the modulus of the magnetic field, e is the elementary charge, Z_e is the charge number (in the special case of electrons, $Z_e = -1$), ψ is the poloidal flux of the magnetic field, R is the major radius and v_φ is the projection of the electron velocity onto the toroidal direction. The second action, J_2 is not very convenient for analytic calculations. This is why we perform a change of variables $\mathbf{J} \to \mathbf{I} = (J_1, \mathcal{H}_{\text{eq}}, J_3)$, where $\mathcal{H}_{\text{eq}}$ is the equilibrium Hamiltonian, representing the energy in the absence of any perturbation. Following Hamilton's equations, the time derivative of the angles is $\dot{\boldsymbol{\alpha}} = \partial_{\mathbf{J}} \mathcal{H} \equiv \boldsymbol{\Omega}$, where we have introduced the three frequencies of motion, satisfying the ordering $\Omega_1 \gg \omega, \Omega_2, \Omega_3$, with ω the frequency of the tearing mode. The distribution function and the Hamiltonian are decomposed into equilibrium and perturbed parts. By definition, the equilibrium quantities do not depend on the angles, but only on the actions. This allows us to linearize the Vlasov equation and, owing to the periodicity of the perturbations with respect to the angles $\boldsymbol{\alpha}$, we can write the perturbed distribution function and Hamiltonian as Fourier series $\{\delta F, \delta \mathcal{H}\} = \sum_{\omega, \mathbf{n}} \{\delta F_{\mathbf{n},\omega}, \delta \mathcal{H}_{\mathbf{n},\omega}\} \exp\left(i\left(\mathbf{n} \cdot \boldsymbol{\alpha} - \omega t\right)\right)$. After some algebra, it can be shown that the exact linear solution of the Vlasov equation is written as

$$\delta F_{\mathbf{n},\omega} = \frac{\partial F_{\text{eq}}}{\partial \mathcal{H}_{\text{eq}}} \delta \mathcal{H}_{\mathbf{n},\omega} + \frac{1}{B} \frac{\partial F_{\text{eq}}}{\partial \mu} \delta \mathcal{H}_{\mathbf{n}',\omega} - \frac{\omega \partial_{\mathcal{H}_{\text{eq}}} F_{\text{eq}} + n_3 \partial_{J_3} F_{\text{eq}}}{\omega - \mathbf{n}^\star \cdot \boldsymbol{\Omega}} \delta \mathcal{H}_{\mathbf{n}^\star,\omega} \tag{4}$$

where $\mathbf{n}' = (n_1 \neq 0, n_2, n_3)$ and $\mathbf{n}^\star = (n_1 = 0, n_2, n_3)$.

The perturbed parallel current is calculated as

$$j_\parallel = eZ_e \int \mathrm{d}^3\mathbf{p} \left(v_{\parallel,\text{eq}} \delta F + \delta v_\parallel F_{\text{eq}}\right) \tag{5}$$

where the perturbed parallel velocity is expressed in terms of the parallel vector potential

$$\delta v_\parallel = -\frac{eZ_e}{m_e} \delta A_\parallel \tag{6}$$

In order to continue further with analytic calculations we assume a Maxwellian equilibrium distribution function

$$F_{\text{eq}} = \frac{n_{\text{eq}}}{\left(2\pi T_{\text{eq}}/m_e\right)^{3/2}} \, \mathrm{e}^{-\frac{\mathcal{H}_{\text{eq}}}{T_{\text{eq}}}} \tag{7}$$

which satisfies $\partial_{\mathcal{H}_{\text{eq}}} F_{\text{eq}} = -F_{\text{eq}}/T_{\text{eq}}$. The perturbed parallel current will be written in normalized units. For this purpose we normalize the velocities to the thermal velocity of elec-

trons v_{th}, the distances to R_0, the frequencies to the transit frequency $\omega_t = v_{\mathrm{th}}/R_0$, the equilibrium distribution function to n_0/v_{th}^3, with n_0 some normalizing density, the parallel vector potential to $B_0 R_0 \rho_\star^2$ and the temperature to a normalizing temperature defined as $T_0 = m_e v_{\mathrm{th}}^2/2$. Using the perturbed distribution function given by Eq. (4) and considering only deeply passing electrons, we show in Appendix B that the perturbed parallel current can be expressed as

$$j_\parallel(\mathbf{x},t) = \rho_\star e n_0 v_{\mathrm{th}} \frac{2}{\hat{T}_{\mathrm{eq}}} \sum_{m,n,\omega} \left\langle \hat{v}_\parallel^2 \frac{\hat{\omega} - \hat{\omega}_{\star g}}{\hat{\omega} - \hat{k}_\parallel \hat{v}_\parallel - \hat{\omega}_D} \right\rangle \delta \hat{A}_{\parallel m,n,\omega}(\mathbf{x})\ \mathrm{e}^{i(m\theta + n\varphi - \omega t)} \tag{8}$$

where m and n are the poloidal and toroidal mode numbers, respectively. The angles have been replaced by θ and φ, representing the poloidal and toroidal angles, respectively. The symbol $\hat{\cdot}$ indicates normalized quantities, the parallel wave vector $k_\parallel$ is given by $k_\parallel = (m/q - n)/R_0$ and the magnetic drift frequency ω_D is given by $\omega_D = 2qn/r \left(m_e v_{\parallel,\mathrm{eq}}^2 + \mu B_0\right)/(e Z_e B_0 R_0)$, with q the safety factor and R_0 and B_0 the major radius and the modulus of the magnetic field, respectively, evaluated both at the magnetic axis. The notation $\langle \cdots \rangle$ has been introduced to represent an average over gyro-centre equilibrium velocity space weighted by the equilibrium distribution function

$$\langle \cdots \rangle = \int \mathcal{J}\, \mathrm{d}v_{\parallel,\mathrm{eq}}\, \mathrm{d}\mu \cdots F_{\mathrm{eq}} \tag{9}$$

Notice that $k_\parallel$ vanishes on the rational surface defined as $q = m/n$. In the remainder of this paper, the eq subscript for the parallel velocity will be dropped for the sake of simplicity. Note that $\rho_\star$ gives the typical ordering between the equilibrium and the perturbed distribution function and $e n_0 v_{\mathrm{th}}$ is the normalization for the current. In this expression we have introduced the generalized diamagnetic frequency $\omega_{\star g} = n T_{\mathrm{eq}} \partial_{J_3} \log F_{\mathrm{eq}}$, which includes all the spatial dependence of the equilibrium. For thermal particles, at lowest order in $\rho_\star$, one can write $J_3 \approx -e Z_e \psi$. Therefore, the derivative with respect to J_3 can be reduced to a derivative with respect to the radial position.

III. GYRO-KINETIC DISPERSION RELATION OF THE TEARING INSTABILITY

In this section, we will use the expression for the perturbed parallel current, given by Eq. (B16), in Ampère's law, given by Eq. (2), to derive the dispersion relation of the tearing instability. Ampère's law can also be written using normalized quantities and projecting onto one single (m,n,ω) Fourier mode

$$\hat{\delta}_e^2 \hat{\nabla}_\perp^2 \delta \hat{A}_{\parallel m,n,\omega}(\mathbf{x}) = \frac{2}{\hat{T}_{\mathrm{eq}}} \left\langle \hat{v}_\parallel^2 \frac{\hat{\omega} - \hat{\omega}_{\star g}}{\hat{\omega} - \hat{k}_\parallel \hat{v}_\parallel - \hat{\omega}_D} \right\rangle \delta \hat{A}_{\parallel m,n,\omega}(\mathbf{x}) \tag{10}$$

where $\hat{\delta}_e = \delta_e/R_0$ and $\delta_e = \sqrt{m_e/\mu_0 e^2 n_0}$ is the electron skin depth. In the following, the $\hat{\cdot}$ symbol will be dropped for the sake of simplicity and all quantities are assumed to be normalized. The dispersion relation of the tearing mode is obtained integrating equation (10), but for this purpose we need to give convenient equilibria that will allow us to perform analytic calculations.

Regarding the equilibrium distribution function F_{eq}, we assume that it is given by the background Maxellian represented in (7), in normalized units it takes the form

$$F_{\mathrm{eq}} = \frac{n_{eq}}{(\pi T_{eq})^{3/2}} \exp\left(-\frac{v_\parallel^2 + v_\perp^2}{T_{eq}}\right) \tag{11}$$

As for the vacuum equilibrium field, we suppose a simplified expression of the magnetic field in cylindrical geometry $\mathbf{B} = B_0 R_0 \left(r/q R_0 \mathbf{e}_\theta + \mathbf{e}_\varphi\right)/R$. The poloidal flux is then written as

$$\psi(r) = B_0 \int_0^r \frac{r'}{q(r')}\, \mathrm{d}r' \tag{12}$$

and therefore its radial derivative is

$$\frac{\mathrm{d}\psi}{\mathrm{d}r} = B_0 \frac{r}{q(r)} \tag{13}$$

the expression for the generalized diamagnetic frequency can be written as follows

$$\begin{aligned}\omega_{\star g} =& \frac{n T_{\mathrm{eq}}}{e} \frac{q}{r B_0} \left[\frac{1}{n_{\mathrm{eq}}} \frac{\mathrm{d}n_{\mathrm{eq}}}{\mathrm{d}r}\right. \\ &\left. + \frac{1}{T_{\mathrm{eq}}} \frac{\mathrm{d}T_{\mathrm{eq}}}{\mathrm{d}r} \left(\frac{v_\parallel^2}{v_{\mathrm{th}}^2} + \frac{\mu B}{T_{\mathrm{eq}}} - \frac{2 v_\parallel u_e}{v_{\mathrm{th}}^2} - \frac{3}{2}\right) + 2 \frac{v_\parallel}{v_{\mathrm{th}}^2} \frac{\mathrm{d}u_e}{\mathrm{d}r}\right]\end{aligned} \tag{14}$$

Note that we keep the electron mean parallel velocity, together with its radial gradient. However, in the following, the assumption is made that $u_e \ll v_{\mathrm{th}}$, so that the term multiplying the temperature gradient simplifies to the standard $E/T_{\mathrm{eq}} - 3/2$. Nevertheless, the gradient ∇u_e is kept. Therefore, the diamagnetic frequency can be split into standard density and temperature terms, $\omega_{\star n}$ and $\omega_{\star T}$, respectively,

and a term coming from the radial gradient of the parallel velocity $\omega_{\star u}$, i.e.

$$\omega_{\star g} = \omega_{\star n} + \omega_{\star T} + \omega_{\star u} \equiv \omega_\star + \omega_{\star u} \tag{15}$$

where the notation $\omega_\star$ has been used to gather both density and temperature gradients. Using normalized quantities, each of these frequencies read

$$\hat{\omega}_\star = \rho_\star n \hat{T}_{\rm eq} \frac{q}{2\hat{r}} \left[\frac{1}{\hat{n}_{\rm eq}} \frac{{\rm d}\hat{n}_{\rm eq}}{{\rm d}\hat{r}} + \frac{1}{\hat{T}_{\rm eq}} \frac{{\rm d}\hat{T}_{\rm eq}}{{\rm d}\hat{r}} \left(\hat{E} - \frac{3}{2} \right) \right] \tag{16}$$

$$\hat{\omega}_{\star u} = \rho_\star n \frac{q}{\hat{r}} \hat{v}_\parallel \frac{{\rm d}\hat{u}_e}{{\rm d}\hat{r}} \tag{17}$$

The mean parallel velocity must be related to the safety factor by the Ampère's law applied to the equilibrium. In the cylindrical limit, Ampère's law in normalized units can be approximated as

$$\frac{\rho_e R_0}{\delta_e^2} \hat{J}_{\rm eq} = \frac{1}{\hat{r}} \frac{\rm d}{{\rm d}\hat{r}} \left(\frac{\hat{r}^2}{q} \right) \tag{18}$$

where the equilibrium current is obtained from the integration of the equilibrium distribution function

$$J_{\rm eq} = e Z_e \int \mathcal{J} \, {\rm d}v_\parallel \, {\rm d}\mu v_\parallel F_{\rm eq} \tag{19}$$

with $\mathcal{J} = 2\pi B/m_e$. The equilibrium parallel current is then $J_{\rm eq} = e Z_e n_{\rm eq} u_e$ and in normalized units

$$\hat{J}_{\rm eq} = Z_e \hat{n}_{\rm eq} \hat{u}_e \tag{20}$$

Unless stated otherwise, all quantities are normalized and thus the $\hat{}$ will be dropped. We assume that the gradient of the equilibrium parallel current is mainly due to the gradient of the mean electron parallel velocity. Therefore, one can integrate the normalized Ampère's law to obtain the expression of the safety factor in terms of the integrated mean velocity

$$q\left(r\right) = \frac{\delta_e^2}{\rho_e R_0 Z_e n_{\rm eq}} \frac{r^2}{\int_0^r {\rm d}r' r' u_e\left(r'\right)} \tag{21}$$

Therefore, the differential equation (10) can be written using only the radial profile of the safety factor, which yields the linear dispersion relation of the tearing mode. Nevertheless, solving analytically this dispersion relation in the whole radial domain for general profiles of density, temperature and electron velocity is rather arduous. Therefore the tearing mode dispersion relation is solved by splitting it into two linear differential equations that will be solved in two different regions of the radial domain: an ideal outer region and a narrow resonant layer. For each region we will make some assumptions. In the resonant layer, $|k_\parallel| \ll 1$ and therefore the whole resonance $\omega - k_\parallel v_\parallel$ must be kept leading to the ordering $\omega \approx k_\parallel v_{\rm th}$, however in the ideal region, $|\omega| \ll |k_\parallel v_\parallel|, |\omega_{\star g}|$. The two solutions are matched by considering the so-called constant-ψ approximation[1] that assumes that the perturbed parallel scalar potential of the magnetic field is constant inside the non-ideal layer.

A. The tearing mode equation in the outer (ideal MHD) region

In the ideal region where $\omega_{\star g} \gg \omega$ and $k_\parallel v_\parallel \gg \omega, \omega_D$ the expression in between brackets of equation (10) reads

$$\left\langle v_\parallel^2 \frac{\omega - \omega_{\star g}}{\omega - k_\parallel v_\parallel - \omega_D} \right\rangle = \left\langle v_\parallel^2 \frac{\omega_\star}{k_\parallel v_\parallel} \right\rangle \tag{22}$$

Since $\omega_\star$ (resp. $\omega_{\star u}$) is an even (resp. odd) function in $v_\parallel$, the only remaining term in the numerator of expression (22) is $\omega_{\star u}$. This leads to the differential equation

$$\delta_e^2 \nabla_\perp^2 \delta A_{\parallel m,n,\omega}\left(\mathbf{x}\right) = -\rho_\star n n_{\rm eq} \frac{q}{r k_\parallel} \frac{{\rm d}u_e}{{\rm d}r} \delta A_{\parallel m,n,\omega}\left(\mathbf{x}\right) \tag{23}$$

Using the relation between the safety factor and the mean electron parallel velocity given by equation (21) and assuming again that the density gradient does not affect significantly the parallel current gradient we can write

$$\frac{{\rm d}^2 A_\parallel\left(r\right)}{{\rm d}r^2} + \frac{1}{r} \frac{{\rm d}A_\parallel\left(r\right)}{{\rm d}r} - \frac{m^2}{r^2} A_\parallel\left(r\right) = \Lambda\left(r\right) A_\parallel\left(r\right) \tag{24}$$

where we have noted $A_\parallel \equiv \delta A_{\parallel m,n,\omega}$ for simplicity and

$$\Lambda\left(r\right) = \frac{-3q'\left(r\right) + 2rq'^2\left(r\right)/q\left(r\right) - rq''\left(r\right)}{r\left(\frac{m}{n} - q\left(r\right)\right)} \tag{25}$$

with q' and q'' representing respectively, the first and second derivatives with respect to r of the safety factor. We consider that $q > 1$, $q' > 0$ and $q'' > 0$ for all r. We will also suppose that there is a radial position r_s such that $q\left(r_s\right) = m/n$. This means that for $r < r_s \Rightarrow q\left(r\right) < m/n$ and for $r > r_s \Rightarrow q\left(r\right) > m/n$. Then, for $r < r_s$ (resp. $r > r_s$) we have the inequality $\Lambda\left(r\right) < 0$ (resp. > 0), which means that for $A_\parallel > 0$ the second derivative must be negative (resp. positive) and therefore the solution is concave (resp. convex). In addition, note that $\lim_{r \to r_s^\pm} \Lambda\left(r\right) = \pm\infty$. This means that the first derivative is discontinuous at the position $r = r_s$, which allows us to define the parameter Δ'[1]

$$\Delta' = \lim_{\varepsilon \to 0} \frac{A'_\parallel(r_s + \varepsilon) - A'_\parallel(r_s - \varepsilon)}{A_\parallel(r_s)} \tag{26}$$

where $A'_\parallel$ denotes the derivative with respect to r of $A_\parallel$. This parameter represents the jump of the solution accross the resonant surface and it will be used as a matching parameter between the solution in the inner region and the solution in the outer region.

Equation (24) can be solved using the shooting method[2] for a general q profile, but in the following we use a q profile of the Wesson-type[3]

$$q(r) = q_a \frac{r^2/\epsilon^2}{1 - (1 - r^2/\epsilon^2)^{\nu+1}} \tag{27}$$

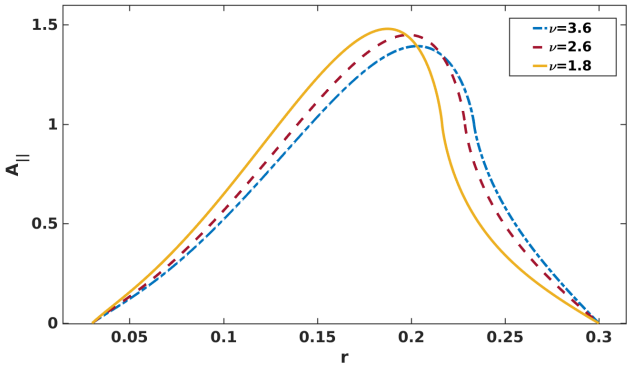

Figure 1: The tearing mode eigenfunction for different values of ν, $q_a = 3.5$ and $\epsilon = 1/3.3$.

where q_a is the value of the safety factor at the position $r = a$ and ν is a parameter that controls the current density peaking. The solution of the tearing mode equation in the outer region is presented in Fig. 1 for three different values of the parameter ν, and fixing $q_a = 3.5$ and the aspect ratio $R_0/a = 0.3$. The boundary conditions $A_\parallel(r_{min}) = A_\parallel(r_{max}) = 0$ are used, and at the resonant surface $r = r_s$, we fix a normalized value $A_\parallel(r_s) = 1$. The fact that the solution is not necessarily symmetric with respect to the resonant surface $r = r_s$ is represented by the parameter

$$\Sigma' = \lim_{\varepsilon \to 0} \frac{A'_\parallel(r_s + \varepsilon) + A'_\parallel(r_s - \varepsilon)}{A_\parallel(r_s)} \tag{28}$$

Although it is not as widely used as Δ', it was shown in resistive MHD[4], that the stability of the tearing mode depends on both Δ' and Σ'. In fact it is shown in Ref. 4 that a tearing mode can be stable even with a positive Δ'. In Fig. 2 we show the contours of Δ' in solid black lines and Σ' in solid red lines scanning over q_a and ν. The magenta lines denote the position of the resonant surface. The dashed blue line presents the limit $q(r_{min}) = 1$. The domain of interest for the analysis of the $(m, n) = (2, 1)$ mode relies above that limit. Beneath it, the mode would co-exist with the $(m, n) = (1, 1)$ mode. In this region the contours of Δ' and Σ' are almost parallel. In the next section we assume that the value of Δ' is known and determined from the outer solution, and we use it to solve the tearing equation in the inner layer.

B. The tearing mode equation in the inner region

In the region around the resonant surface $k_\parallel \ll 1$ and therefore the resonance in the expression in between brackets of Eq. (10) is kept as it is. Due to parity reasons, the contribution from $\omega_{\star u}$ in the numerator can be neglected, so that the

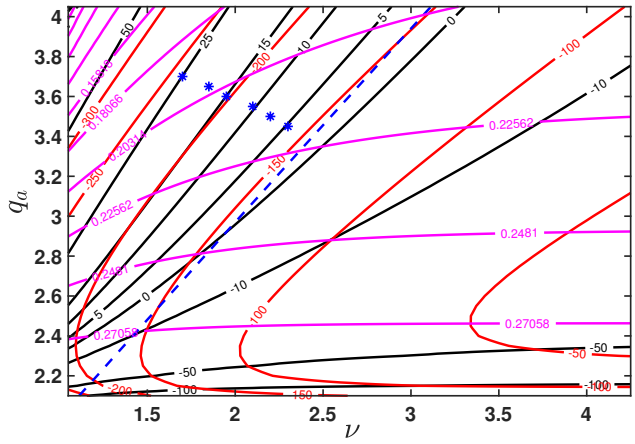

Figure 2: Contours of Δ' (black), Σ' (red) and the resonant surface position r_s (magenta) as a function of the q profile parameters ν and q_a. The blue dashed line denotes the limit $q(r_{\min}) = 1$ and the blue asterisks denote the parameter of the simulations that will be shown in section V.

tearing mode equation reads

$$\delta_e^2 \nabla_\perp^2 \delta A_{\parallel m,n,\omega}(\mathbf{x}) = \frac{2}{T_{\rm eq}} \left\langle v_\parallel^2 \frac{\omega - \omega_\star}{\omega - k_\parallel v_\parallel - \omega_D} \right\rangle \delta A_{\parallel m,n,\omega}(\mathbf{x}) \tag{29}$$

We assume that the widht of the resonant layer is 2Δ. Integrating the equation over this region yields

$$\delta_e^2 \int_{-\Delta}^{\Delta} \frac{\mathrm{d}^2 A_\parallel}{\mathrm{d}x^2}\, \mathrm{d}x = A_\parallel(0) \int_{-\Delta}^{\Delta} \Lambda\, \mathrm{d}x \tag{30}$$

where we have again noted $A_\parallel \equiv \delta A_{\parallel m,n,\omega}$ and the so-called constant-ψ approximation has been made, assuming that the solution is constant in the resonant layer. In addition, to perform the integration in the resonant layer the assumption of slab geometry is made, such that $\nabla_\perp^2 \equiv \mathrm{d}^2/\,\mathrm{d}x^2$, where $x = (r - r_s)/R_0$ represents the distance to the rational surface at the radial position r_s, normalized to R_0. This assumption is justified due to the small width of the resonant layer. Moreover, the coefficient Λ is now given by the more general expression

$$\Lambda = \frac{2}{T_{\rm eq}} \left\langle v_\parallel^2 \frac{\omega - \omega_\star}{\omega - k_\parallel v_\parallel - \omega_D} \right\rangle \tag{31}$$

The integral on the left hand-side of Eq. (30) gives $\Delta' A_\parallel(0)$. For the integral on the right-hand side we perform a change of variable $v'_\parallel = -v_\parallel$ and $x' = -x$ to the negative domain of the space integral. In addition, since the perturbed parallel current is localised in a very narrow region around the resonant surface, we can extent the integral with respect to the radial distance to infinity without introducing significant errors. Under these assumption, the collisionless tearing

mode dispersion relation in the magnetic limit is expressed in normalized units as

$$\delta_e^2\,\Delta' = \frac{8n_{eq}}{T_{eq}^{5/2}\sqrt{\pi}}\int_0^{+\infty}\mathrm{d}x\int_{-\infty}^{+\infty}\mathrm{d}v_\parallel\int_0^{+\infty}v_\perp\,\mathrm{d}v_\perp v_\parallel^2\,\mathrm{e}^{-\frac{v_\parallel^2+v_\perp^2}{T_{eq}}}\frac{\omega-\omega_\star}{\omega-k_\parallel(x)v_\parallel-\omega_D} \tag{32}$$

In this expression, the parallel wave vector can be expressed as $k_\parallel(x) = k_y/L_s x = k'_\parallel x$, with L_s the magnetic shear scale length and $k_y = m/r$, and the diamagnetic frequency is expressed as

$$\omega_\star = \omega_{\star n}\left[1+\eta_e\left(v^2-\frac{3}{2}\right)\right] \tag{33}$$

where $v^2 = v_\parallel^2 + v_\perp^2$, $\omega_{\star n} = \rho_\star n T_{\mathrm{eq}} q/2r\, n'_{eq}/n_{eq}$ and $\eta_e = \left(n'_{\mathrm{eq}}/n_{\mathrm{eq}}\right)/\left(T'_{\mathrm{eq}}/T_{\mathrm{eq}}\right)$.

IV. ANALYTICAL SOLUTION OF THE TEARING MODE DISPERSION RELATION

It is not straightforward to compute the integral (32). In order to shed some light of the underlying physics, we make first of all the assumption that all the particles are deeply passing. Afterwards, we assume that a fraction of the electron population is deeply trapped and analyse its effect on the tearing instability.

A. Solution of the dispersion relation with only passing particles

As a first step, we neglect the curvature and gradient of the magnetic field, such that $\omega_D = 0$ and only the $k_\parallel v_\parallel$ resonance is taken into account, i.e. the resonance with the parallel motion ($\omega - k_\parallel v_\parallel$). In this case, since the denominator does not depend on the perpendicular velocity, we can first of all perform the integral with respect to $v_\perp$. Secondly, the velocity space integral can be performed using the plasma dispersion function and its derivatives as defined in Ref. 5.

After some algebra, the dispersion relation of the tearing mode reads

$$i\delta_e^2\Delta' = \frac{4n_{eq}\sqrt{\pi}}{\sqrt{T_{eq}}|k'_\parallel|}\left[\omega-\omega_{\star n}\left(1+\left(2T_{eq}-\frac{3}{2}\right)\eta_e\right)\right] \tag{34}$$

Writing $\omega = \omega_r + i\gamma$, where ω_r is the real frequency and γ is the growth rate, the solution of Eq. (34) reads

$$\gamma = \frac{1}{4\sqrt{\pi}}\frac{\sqrt{T_{\mathrm{eq}}}}{n_{\mathrm{eq}}}\delta_e^2|k'_\parallel|\Delta' \tag{35}$$

$$\omega_r = \omega_{\star n}\left[1+\left(2T_{eq}-\frac{3}{2}\right)\eta_e\right] \tag{36}$$

Strictly speaking, if one chooses the normalization constant T_0 as the value of the temperature at the resonant surface, in this case $T_0 = T_{eq}$ i.e. $\hat{T}_{eq} = 1$, then the background density and temperature profiles do not change the growth rate of the mode, however they additionally make the mode oscillate with a real frequency that scales linearly with the density and temperature gradients. It is important to note that we have taken into account density and temperature gradients in the local approximation. This means that although we consider radial profiles of the background quantities, they are evaluated locally, so they enter the equation as a constant value on the resonant surface. Of course, a more rigorous approach is to consider the profiles. However this makes the x-integral far too complicated to be solved analytically. The effect of profiles will be evaluated more adequately in the next section with a numerical code.

We look now into the effects of the inhomogeneity of the magnetic field on the stability of the tearing mode. This means that the term containing the toroidal effects are kept in the resonant term of Eq. (32). Of course, the concept of toroidicity in slab geometry is quite contradictory. In fact, several assumptions are made for the magnetic drift ω_D. First, we consider the local approximation, meaning that the x-dependence is omitted but the derivative with respect to x can be non-zero. Therefore, the geometry term $\mathbf{b}\times\nabla\mathbf{B}$ responsible for the curvature of the magnetic field can be treated as a parameter in the equation. Second, all oscillations in the perpendicular direction are neglected, we assume to be at the low field side of the tokamak where $\theta = 0$. Thus the toroidal coupling between modes is not considered.

Integrating first over the radial direction allows to make no assumption on the dependence of ω_D on the velocity space. Then using the well known gaussian integrals for the velocity space, we obtain the same expressions for the frequency and growth rate as those given by Eq. (35). A more accurate calculation can be performed by considering that the magnetic drift is actually a differential operator in the poloidal angle, which introduces nonloncal effects due to mode-mode coupling. It can be shown that even when these effects are taken into account, the mode frequency and growth rate are not modified. The details of the calculations are not given here for the sake of readiness and clarity, but the interested reader can find the complete calculation in Appendix D.

Therefore, when considering only passing particles, and in the collisionless magnetic limit, the drift of particles due to the magnetic field inhomogeneity does not have an impact on

the stability of the mode.

B. Correction due to the presence of trapped electrons

To consider the impact of trapped electrons on the stability of the tearing mode, we need to use the resonant response given by expression (4), which is the one valid for both passing and trapped electrons, since no assumption on their orbits were made at that step. For trapped particles, $\Omega_2 \gg \omega, \Omega_3$. Therefore, for a resonance to occur the only possibility is $n_2 = 0$. This is mathematically equivalent to performing a bounce-average of the Vlasov equation. The resonance then reduces to $\omega - n_3\Omega_3$. In Appendix C we show that for trapped particles, the precessional frequency is proportional to the magnetic drift (see Eq. (C30)). In the absence of magnetic drift the response of trapped particles to the tearing mode is purely non resonant. Therefore, trapped particles do not contribute to the growth rate and the response of the whole electron population is reduced to the response of deeply passing electron. Note that even if the response was resonant, it can be shown (see Appendix E) that the Hamiltonian of deeply trapped particles in the absence of magnetic drift vanishes. Thus, the velocity integral in Eq. (32) must be performed only in the passing domain $|v_\parallel| > \sqrt{2\varepsilon}\,|v_\perp|$ and the growth rate and frequency finally read

$$\gamma = \frac{\delta_e^2\,|k_\parallel'|}{2\sqrt{\pi}}\,\frac{T_{eq}^{3/2}}{n_{eq}}\,\Delta'\,(1+2\varepsilon) \tag{37}$$

$$\omega = \omega_{\star n}\left[1 + \left(2T_{eq} - \frac{3}{2}\right) n_{eq}\right] \tag{38}$$

Therefore, when a fraction of the electron population is magnetically trapped, the growth rate of the tearing mode is increased by a factor $1 + 2\epsilon$. Physically, this can be understood as follows. The free energy for the tearing mode to be excited comes from the radial gradient of the equilibrium parallel current. This free energy is encapsulated in the stability parameter Δ'. Therefore, the free energy comes from the ideal region outside the resonant layer. This energy is subsequently transferred to particles within the resonant layer, where kinetic effects must be retained. The difference between the free energy that the mode takes from the idea region and the energy that the mode transfers to the particles in the resonant layer is the energy available for the mode to grow. Since deeply trapped electrons do not contribute to this transfer of energy, there is an increase of energy available for the mode to grow, resulting in an increased growth rate.

When the magnetic drift is taken into account, a resonance can occur between the tearing mode and the precessional motion of trapped particles, opening a new channel of energy transfer from the mode to the particles and therefore stabilizng the mode. The analytic calculation of the modification of the growth rate in the presence of trapped particles and magnetic drift is not straightforward. Therefore, we use a gyro-kinetic code for the remaining analysis.

V. LINEAR GYROKINETIC SIMULATIONS OF COLLISIONLESS TEARING MODES WITH GKW

The self-consistent treatment of tearing modes requires a radial profile in geometry and physical quantities. For this reason, the global version of the gyrokinetic code GKW[6] is used. In this section we provide a brief description of the code and then we present the implementation of the tearing mode instability in GKW.

A. The gyrokinetic model in GKW

The code GKW solves a set of gyrokinetic equations. The full details can be found in Ref. 6 and references therein. Here we outline the basic set of linear equations that are solved. As in our theoretical approach presented in the previous sections, the δF approximation is used. The equation for the perturbed distribution function, for each species is,

$$\frac{\partial g_s}{\partial t} + \left(v_\parallel \mathbf{b} + \mathbf{v}_D\right)\cdot\nabla\delta F_s - \frac{\mu_s}{m_s}\frac{\mathbf{B}\cdot\nabla B}{B}\frac{\partial \delta F_s}{\partial v_\parallel} = S\left(F_{\mathrm{eq},s}\right) \tag{39}$$

where $g_s = \delta F_s + (Z_s e/T) v_\parallel \langle A_\parallel \rangle F_{\mathrm{eq},s}$, $\mu = m_s v_\perp^2/2B$ is the magnetic moment, $v_\parallel$ is the velocity along the magnetic field, and m_s and Z_s are, respectively, the particle mass and charge number for species s. The drift velocity due to the gradient and curvature of the magnetic field is $\mathbf{v}_D = (1/Z_s e)(m_s v_\parallel^2 + \mu_s B)/B\mathbf{B}\times\nabla B/B^2$. Note that the nonlinear term ($\mathbf{v}_{E\times B}\cdot\nabla g_s$, where $\mathbf{v}_{E\times B}$ is the $\mathbf{E}\times\mathbf{B}$ velocity) is not taken into account in this linear study. $S\left(F_{\mathrm{eq},s}\right)$ is the source term which is determined by the species s equilibrium distribution function. The last term of the left-hand side of Eq. (39) is responsible for the trapping of particles (the so-called μ-grad$B$ or mirror term). The temperature and density profiles have the radial form,

$$n(r) = n_0 \exp\left[-\frac{R}{L_n} w \tanh\left(\frac{r-r_0}{w}\right)\right] \tag{40}$$

$$T(r) = T_0 \exp\left[-\frac{R}{L_T} w \tanh\left(\frac{r-r_0}{w}\right)\right] \tag{41}$$

where the distances are normalised to R_0, w is the width of the region where the gradient is localised, R/L_n, R/L_T, n_0 and T_0 are the logarithmic density and temperature gradients and the density and temperature, respectively, all evaluated at the reference radius r_0. All the normalizations in the code are consistent with the ones used so far in the present paper. The electrostatic potential is calculated from the gyrokinetic

quasineutrality equation given by,

$$\sum_s Z_s e \int (J_0 \cdot \delta F_s)^\dagger \, \mathcal{J}_s \, \mathrm{d}v_\parallel \, \mathrm{d}\mu_s + \sum_s \frac{Z_s^2 e^2}{T_s} \int \left(\left(J_0^2 \cdot \delta F_s \right)^\dagger - \phi \right) F_{\mathrm{eq},s} \mathcal{J}_s \, \mathrm{d}v_\parallel \, \mathrm{d}\mu_s = 0 \quad (42)$$

where the first term is the perturbed charge density and the second is the polarisation density which is only calculated from the local Maxwellian. In this expression, J_0 is the gyro-average operator and the dagger symbol represents its conjugate. Similarly, the parallel vector potential is calculated from parallel Ampère's law

$$-\nabla^2 A_\parallel + \sum_s \frac{\mu_0 Z_s^2 e^2}{T_s} \int v_\parallel^2 \left(J_0^2 \cdot A_\parallel \right)^\dagger F_{\mathrm{eq},s} \mathcal{J}_s \, \mathrm{d}v_\parallel \, \mathrm{d}\mu_s = \sum_s \frac{\mu_0 Z_s e}{T_s} \int v_\parallel \left(J_0 \cdot g_s \right)^\dagger \mathcal{J}_s \, \mathrm{d}v_\parallel \, \mathrm{d}\mu_s \quad (43)$$

B. Simulations set-up to analyse the tearing instability in GKW

The tearing mode is linearly excited in the code[7] by introducing an electron flow u_e in the equilibrium distribution function. The generated tearing mode is driven due to the inertia of electrons when we neglect resistivity through collisions. The mean velocity of electrons is related to the imposed q profile following the expression (21). We use the same q profile as for our analytic calculations, given by the Eq. (27). As an example, a linear collisionless simulation of a self-consistent tearing mode has been run for the following parameters: aspect ratio $R_0/a = 3.33$, normalized ion Larmor radius $\rho_\star = \rho_i/R_0 = 0.002815$, the safety factor at the edge $q_a = 3.5$, current peaking parameter $\nu = 2.6$. This corresponds to a tearing mode with $\Delta' \approx 0.99$, calculated using the shooting method to solve the tearing equation outside the resonant layer, as presented in section III A. We represent in Fig. 3 the safety factor profile described by Eq. (27) (bottom) for these parameters, the radial eigenfunction of the parallel vector potential (middle) and its second radial derivative (top) which is highly localized around the resonant layer at the $q(r/R_0) = 2$ surface, represented by a vertical dashed line together with the label $r = r_s$. For linear simulations, a single $n = 1$ toroidal mode is considered and the numerical resolution is $N_r \times N_s \times N_{v_\parallel} \times N_\mu = 512 \times 30 \times 64 \times 15$, where N_r is the number of radial grid points, N_s is the number of points in the parallel direction, $N_{v_\parallel}$ is the number of points in parallel velocity and N_μ is the number of points in the magnetic moment direction. The selected number of points in the radial direction are enough to describe the physics around the thin resonant layer[7]. In our collisionless simulations we can artificially suppress the electrostatic potential, the mirror term and the curvature of the magnetic field. This capability allows us to run the code in the same limit as the one where the analytic theory has been derived. When radial gradients are used in the simulations, the reference position r_0 is the same as the position of the resonant surface, i.e. $r_0 = r_s$, and the width of the region where the gradient is localized is set to $w = 0.03$.

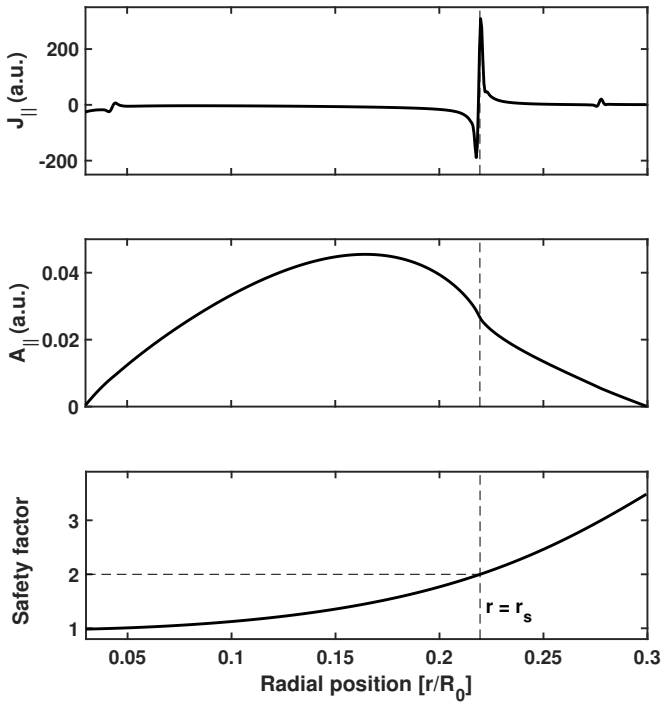

Figure 3: The radial profiles of the imposed safety factor q (bottom), the parallel vector potential (middle) and its radial second derivative (top) as calculated by GKW in toroidal geometry for density and temperature gradients $R/L_n = R/L_T = 2.2$. The most unstable mode locates at the $q = 2$ surface, indicated by a vertical dashed line and labeled by $r = r_s$, where the parallel current is highly localized.

C. Parametric study of the collisionless tearing mode

Analytically, we have shown previously that, when particle trapping is taken into account, the growth rate is increased by a factor $1 + 2\epsilon$. The position of the resonant surface is inversely proportional to Δ'. This means that including trapping effects will amplify the growth rate by a ~ 1.44 factor that should decrease with Δ'. In Fig. 4, we represent the ratio between the tearing mode growth rate with and without trapping as a function of the stability parameter Δ', calculated using the shooting method and the q profile used in

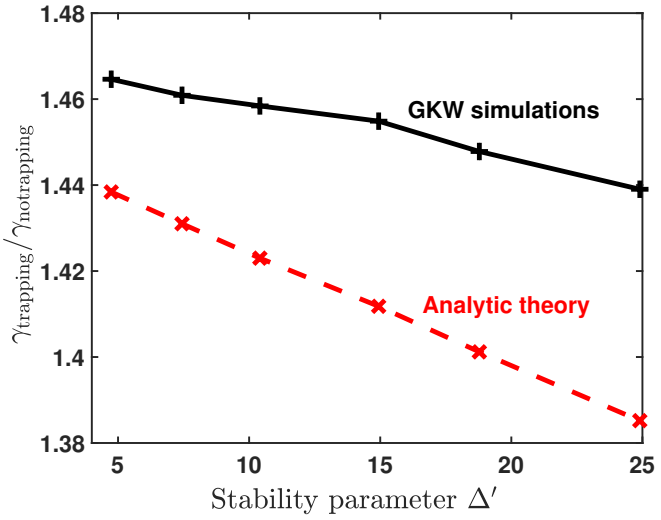

Figure 4: The ratio between the growth rate with and without trapping in terms of Δ', in solid black line as calculated numerically with GKW and in red dashed line as predicted by our analytic theory.

GKW. The scan on Δ' has been performed by changing the q_a and ν parameters in the q profile. The points used in this scan are indicated by asterisks in Fig. 2. The analytical prediction in dashed red line agrees with the numerical calculation from GKW simulations, represented by solid black line, with an error of $\sim 1-5\%$. One can conclude that in the absence of curvature of the field, magnetic trapping destabilizes the mode by a factor that depends on the position of the resonant surface of the mode.

We have subsequently performed a parametric study of the linear instability of the tearing mode to further study the impact of the curvature, radial gradients and particle trapping. For this purpose, we have run a set of global simulations, with and without temperature gradient, with and without particle trapping and with and without magnetic curvature. Note that the density gradient is always set to $R/L_n = 0$. This is due to the fact that the equilibrium parallel current depends linearly on the density. Therefore, in the absence of density gradient the stability parameter Δ' is not modified.

The growth rate in the absence of temperature gradient is presented in Fig. 5. The calculated growth rate is plotted as a function of Δ' on the top panel and $|k'_\parallel|\Delta'$ on the bottom panel. The black curves represent the case of no particle trapping, neglecting (solid) and taking into account (dashed) the curvature of the magnetic field. These curves are conveniently labeled in the figure. For the sake of readiness, the same labels, colours and symbols are used in the following. As predicted by theory, in the absence of particle trapping, the two curves with/without magnetic curvature overlap in the case of flat density and temperature profiles. When trapping

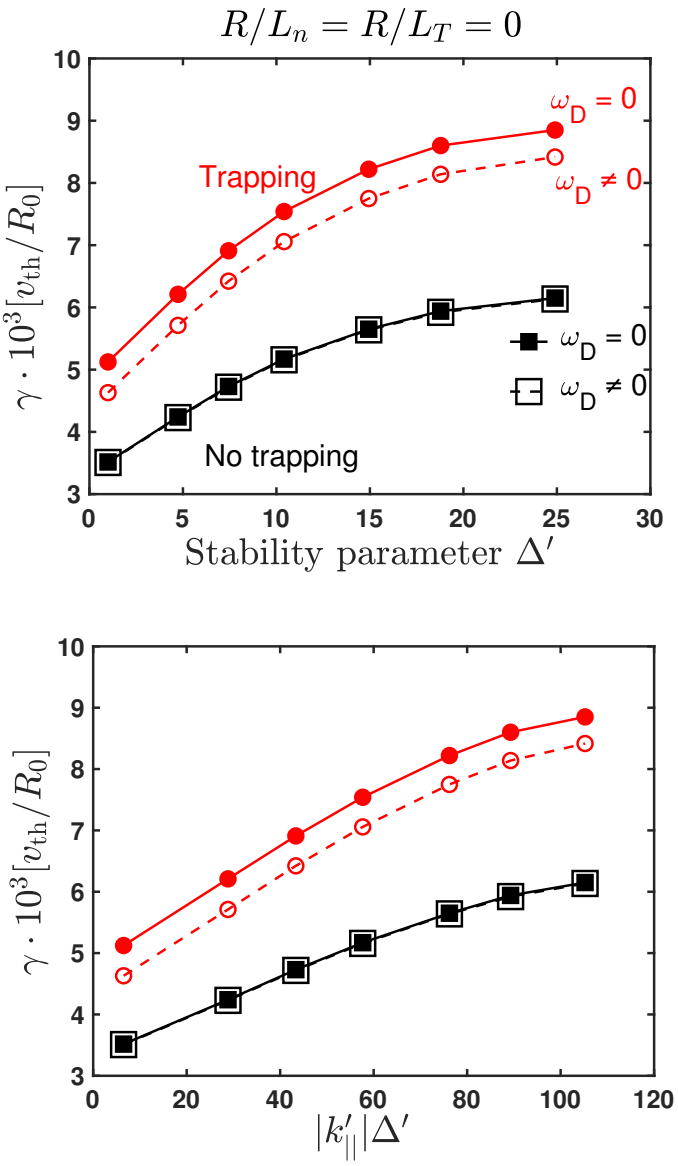

Figure 5: The growth rate of a collisionless tearing mode for flat background profiles as a function of Δ' (top) and $|k'_\parallel|\Delta'$ (bottom) given by GKW simulations, for several cases of a population consisting of only passing particles, and passing and trapped particles and neglecting/considering magnetic curvature.

is considered, the collisionless tearing mode is more unstable, which is consistent with Fig. 4. In that case, it is observec that the magnetic field curvature stabilizes the mode. The reason for this effect is analysed in section VI B.

Regarding the dependence on the stability parameter, our analytic theory predicts a linear scaling of the growth rate with Δ', regardless of the pressure profile. We observe that the trend of the curve with Δ' is linear only for small values

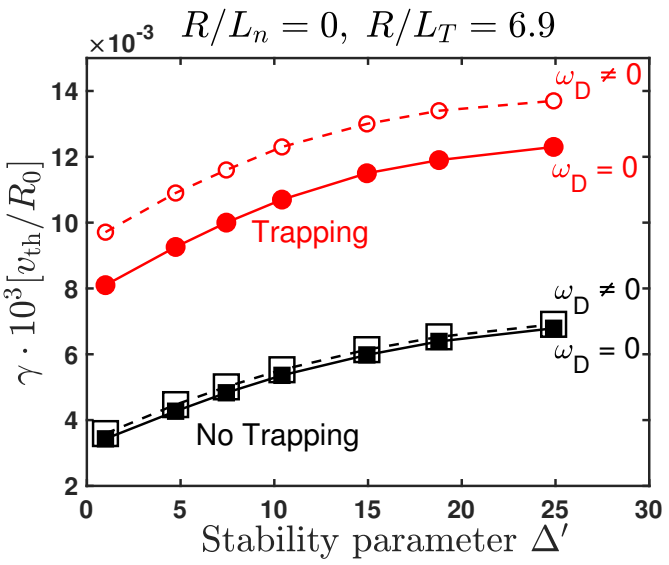

Figure 6: The growth rate of a collisionless tearing mode for a flat density gradient and a non zero temperature gradient ($R/L_T = 6.9$) as a function of Δ' given by GKW simulations, for several cases of a population consisting of only passing particles, and passing and trapped particles and neglecting/considering magnetic curvature.

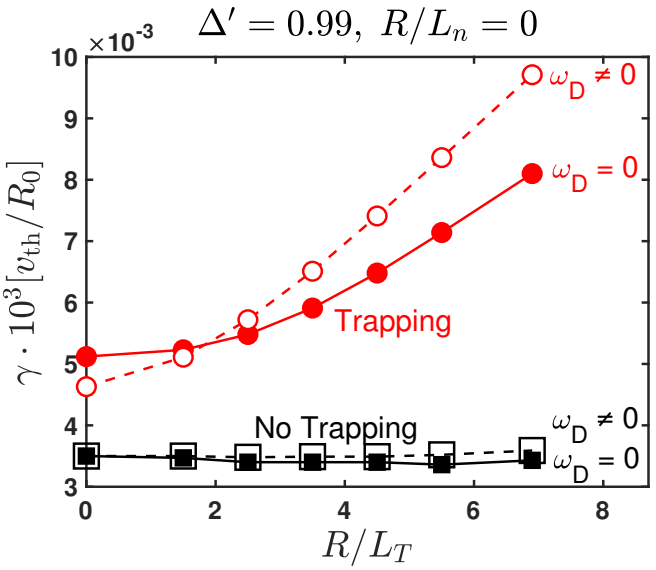

Figure 7: The growth rate of a collisionless tearing mode as a function of Δ' for flat temperature and density profiles.

of Δ' and departs from the linear behaviour when increasing Δ'. Actually, when modifying Δ', the position of the resonant surface is also modified and so is the value of $|k'_\parallel|$, which implies that the proportionality coefficient is modified. However, when looking at the dependence of the growth rate on $|k'_\parallel|\Delta'$, a linear behaviour is observed, which is in better agreement with the analytical relation found in section IV.

Note nonetheless, that a nonlinear behaviour of the growth rate was reported in Ref. 8, where the growth rate was found to scale as $\sqrt{\Delta'}$. This behaviour was explained by the short wavelength effects taken into account in the Bessel function $J_0(k_\perp \rho_e)$. The Bessel function was then expanded for large arguments, and a scaling of the growth rate with $\sqrt{\Delta'}$ and $(\rho_e a)^{1/4}$ was found. The latter is a finite Larmor radius effect. However when we eliminate the finite Larmor radius effect in the code, by not computing the gyroaverage, we have not observed any change in the growth rate of the mode. The effect of variations of the wave vector in the radial direction cannot be verified *per se* in our simulations since a Fourier representation is used for the binormal coordinate (perpendicular to the field) and we consider only one binormal mode. One would need to consider more than a single mode to check this effect, which is left for a future publication.

When temperature gradient is included, the growth rate is amplified with respect to the case $R/L_T = 0$ only when considering the particle trapping. If particle trapping is neglected, the impact of the temperature gradient is negligible. This is shown in Fig. 6, where the dependence of the growth rate on the stability parameter Δ' is plotted considering a temperature gradient $R/L_T = 6.9$. It is observed that the effect of the magnetic drift frequency is opposite to that in the absence of temperature gradient, i.e. the magnetic curvature tends to destabilize the collisionless tearing mode. This is in agreement with recent analytic results based on a fluid approach[9], which suggests an interchange-like destabilization of the collisionless tearing mode.

We have seen that, in the presence of particle trapping, for $R/L_T = 0$ (resp. $R/L_T = 6.9$), the magnetic curvature stabilizes (resp. desctabilizes) the mode. This implies that there must exist a temperature gradient at which the interchange destabilization **??** compensates for the stabilization observed in Fig. 5. To analyse this more in detail we have selected one single Δ' and we have performed a scan on the temperature gradient R/L_T. The result is shown in Fig. **??**. It is observed that, when neglecting the particle trapping, the temperature gradient does not have any significant impact on the tearing mode stability. However, when some particles are trapped, the temperature gradient destabilizes the mode. This destabilization is further increased by the magnetic field curvature only beyond an R/L_T-threshold around $R/L_T \approx 2$.

For the sake of completeness, we have run simulations with flat density and temperature profiles, but considering the electrostatic potential by solving the quasi-neutrality equation, coupled to the gyrokinetic Vlasov-Ampère system. We show the results in Fig. 8, We confirm that including trapping effects destabilizes the mode even in the presence of electrostatic potential. We confirm also a stabilizing role for the curvature in the case of zero gradients, even when the desta-

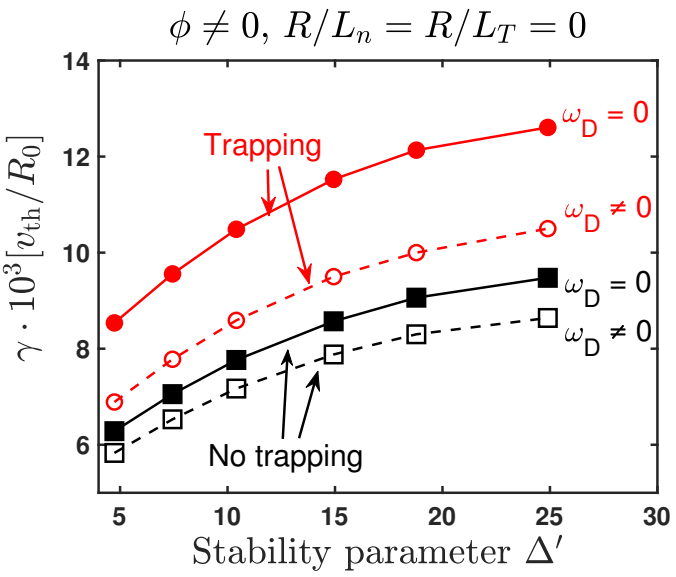

Figure 8: The growth rate of a collisionless tearing mode as a function of Δ' for flat temperature and density profiles.

bilizing effect[10] of the electrostatic potential is considered.

We can see that the role of magnetic field curvature through particle trapping is to stabilize the mode when no gradients are considered, and to destabilize it when temperature gradients are considered, beyond an R/L_T-threshold. This threshold occurs when a stabilizing effect due to trapped particles is compensated by the interchange destabilization. To get a better understanding of the underlying physics, a quantitative analysis of the energy exchange between the particles and the mode has been made by using a diagnostic that computes the variation the kinetic energy of particles in the code.

VI. ENERGY EXCHANGE DIAGNOSTIC FOR WAVE-PARTICLE INTERACTION

The following diagnostic is used to identify in velocity space the various contributions of passing and trapped particles to the linear growth rate of the most unstable mode. It is based on the energy conservation property of the Vlasov-Poisson system of equations which allows to directly link the mode growth rate to the work done by the perturbed electric field on the particles. Strictly speaking, this method is only applicable if the set of equations solved and their numerical implementation conserves energy.

A. Conservation of energy

The time variation of the space-integrated potential energy of an electromagnetic wave is given by

$$\frac{\mathrm{d}\mathcal{E}_p}{\mathrm{d}t} = \frac{\mathrm{d}}{\mathrm{d}t}\int \mathrm{d}^3\mathbf{x}\left(\frac{\epsilon_0}{2}\mathbf{E}\cdot\mathbf{E} + \frac{\epsilon_0 c^2}{2}\mathbf{B}\cdot\mathbf{B}\right) = \int \mathrm{d}^3\mathbf{x}\left(\epsilon_0\mathbf{E}\cdot\frac{\partial\mathbf{E}}{\partial t} + \epsilon c^2\mathbf{B}\cdot\frac{\partial\mathbf{B}}{\partial t}\right) \tag{44}$$

Using Faraday's induction law $\nabla\times\mathbf{E} = -\partial_t\mathbf{B}$ and Ampère's law $\nabla\times\mathbf{B} = \mu_0\mathbf{J} + \mu_0\epsilon_0\partial_t\mathbf{E}$, where $\mathbf{E}$, $\mathbf{B}$ and $\mathbf{J}$ are the electric field, the magnetic field, and the current density, respectively, Eq. (44) becomes

$$\frac{\mathrm{d}\mathcal{E}_p}{\mathrm{d}t} = -\int \mathrm{d}^3\mathbf{x}\left[\mathbf{J}\cdot\mathbf{E} - \frac{1}{\mu_0}\nabla\cdot(\mathbf{E}\times\mathbf{B})\right] \tag{45}$$

Owing to the conservation of the total energy of the system, we have

$$\frac{\mathrm{d}\mathcal{E}_k}{\mathrm{d}t} = -\frac{\mathrm{d}\mathcal{E}_p}{\mathrm{d}t} \tag{46}$$

where $\mathcal{E}_k$ is the kinetic energy of particles. This gives the time evolution of the kinetic energy

$$\frac{\mathrm{d}\mathcal{E}_k}{\mathrm{d}t} = -\sum_s \int \mathrm{d}^3\mathbf{x}\,\mathrm{d}^3\mathbf{v}\; Z_s e\, F_s\;\mathbf{v}\cdot\left(\nabla\widetilde{\phi} + \frac{\partial\widetilde{A}_\parallel}{\partial t}\mathbf{b}\right) + \int \mathrm{d}^3\mathbf{x}\,\frac{1}{\mu_0}\nabla\cdot(\mathbf{E}\times\mathbf{B}) \tag{47}$$

The sign of the time evolution of the kinetic energy indicates the contribution to the growth rate of the mode. If $\dot{\mathcal{E}}_k > 0$, the energy is transferred from the mode to the particles and therefore the mode is damped. In the opposite case, the mode gains energy and is therefore unstable. It is important to note that in the case of global modes such as tearing modes, a positive variation of the particles kinetic energy at a local point does not necessarily suggest destabilization of the whole mode. Some transport of energy should be taken into account through advection, especially when the electrostatic potential is considered and the $\nabla\cdot(\mathbf{E}\times\mathbf{B})$ term is non zero. In our simulations, we check that even when the electrostatic potential is taken into account that term is negligible compared to the $\mathbf{J}\cdot\mathbf{E}$ term. We have implemented in the code the first term on the right hand-side of Eq. (47) as a function of $(r, v_\parallel, v_\perp)$. The last term on the left hand-side is calculated in a separate diagnostic that computes all the radial flows. The implemented diagnostic reads

$$\dot{\mathcal{E}}_k = -eZ_s\int \mathrm{d}sF\left(v_\parallel\mathbf{b} + \mathbf{v_E} + \mathbf{v_D}\right)\cdot\left(\nabla J_0\cdot\phi + \partial_t J_0\cdot A_\parallel\mathbf{b}\right) \tag{48}$$

B. Response of the particles to the tearing mode

We present the results from the described diagnostic, which allows us to characterize the particle response to the collisionless tearing instability in the purely magnetic case, i.e. the electrostatic potential is set to zero and therefore the $\mathbf{E}\times\mathbf{B}$ flux in Eq. (47) vanishes. The local interaction between the waves and particles in the velocity space can thus be described by Eq. (48) with the $A_\parallel$ term only.

Fig. 9 illustrates the local exchange of energy between particles and the mode in the velocity space for $R/L_n = R/L_T = 0$. The plots are shown for a local point around the resonant position $r = r_s$ where the exchange of energy is the most localized. The dashed line in the middle panel denotes the trapping cone $v_\parallel = \sqrt{2r_s/R_0}v_\perp$. As discussed earlier, this relation is valid only at the tokamak midplane where the magnetic field intensity has a maximum value. Therefore, one needs to be aware of the position on the magnetic field when setting the trapping boundary. In our simulations, the amplitude of the mode is localized at $s = 0$, which makes this relation valid. The three different panels represent the three different curves that we have shown in Fig. 5 (actually we have four curves, but when there is no particle trapping the two black curves are the same). It is observed that when trapping is considered without magnetic curvature the effect is the suppresion of the particle response inside the trapping cone, as predicted by our analytic theory. This leads to a decreasing energy transfer from the tearing mode to particles, resulting in an increased growth rate. However, when including magnetic curvature and trapping is allowed, trapped particles respond to the presence of the tearing mode, allowing this way the transfer of energy from the tearing mode to the trapped particles, which results in a decrease of the growth rate. This is evidenced by the bottom panel, where the red curve represents the positions in velocity space at the resonant surface where the precession frequency of trapped particles equals the tearing frequency, i.e. $\omega = n_3\Omega_3\left(v_\parallel, v_\perp\right)$, with $n_3 = 1$. The frequencies of motion are calculated in detail in Appendix C. In particular, we use the expression C30 to plot the red curve. It is observed that the maximum of the response is located on the red curve and corresponds to barely trapped particles. Consequently, one can assess that adding particle trapping in the presence of magnetic curvature can modify the stability of the mode through the resonance between the tearing mode and barely trapped particles.

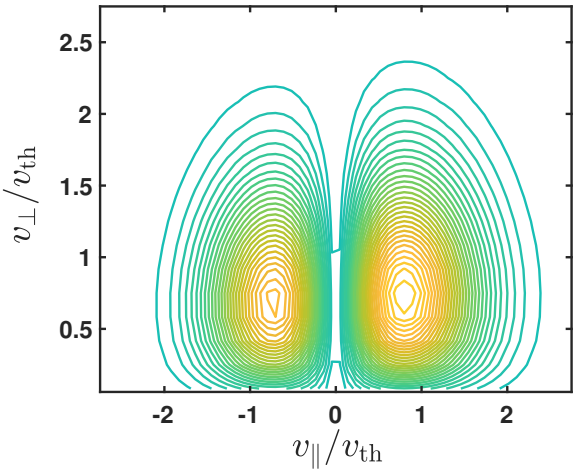

(a) Without particle trapping.

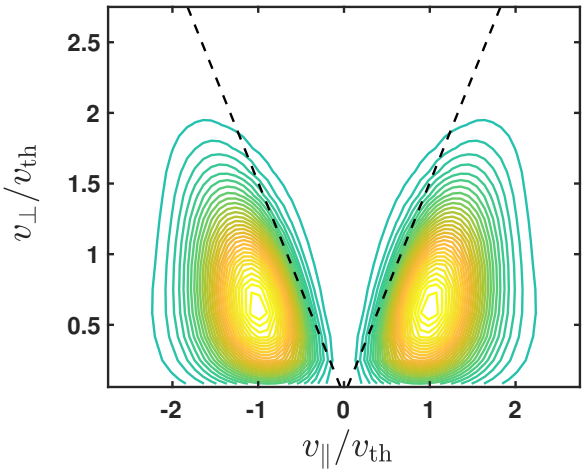

(b) With particle trapping and $\omega_D = 0$.

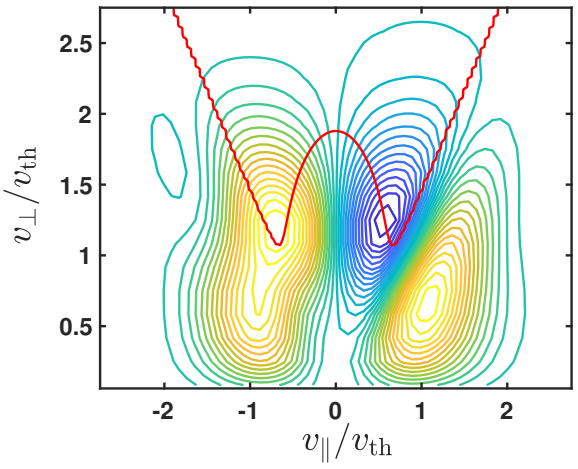

(c) With particle trapping and $\omega_D \neq 0$.

Figure 9: Particle response in the presence of a collisionless tearing mode without density/temperature gradients, i.e. $R/L_n = R/L_T = 0$.

VII. CONCLUSIONS

In this paper we have studied the stability of a collisionless tearing mode in a curved and inhomogeneous magnetic field. The tearing mode equation is derived in the framework of gyrokinetic theory with a Hamiltonian approach. We have found a unique equation that can be used to solve the tearing instability in both the outer (ideal or non-resonant) and inner

(non-ideal or resonant) regions. Using the gyrokinetic theory in the analysis of the tearing mode allows us to look into the kinetic aspects of the instability. This means analyzing possible resonances between particles and the mode in the inner region. In the outer region, the fluid limit is used to avoid the resonances. A shooting method has been employed to integrate the equation of the tearing mode for a general safety factor profile and a diagram of the stability parameter Δ' has been obtained.

We have solved analytically the equation of the tearing mode in the inner region, where the kinetic effects are kept and we have recovered the result that the growth rate scales linearly with $|k'_\parallel|\Delta'$, where $k'_\parallel$ is the radial derivarive of the parallel wave-vector evaluated at the resonant surface. We have also found that trapping effects in the absence of magnetic curvature lead to an increase of the growth rate by a factor $1+2\epsilon$, where $\epsilon = r/R_0$. This is due to the fact that the mode transfer its energy mainly to passing electrons in the resonant layer. Therefore, introducing trapped electrons increases the energy available for the mode to grow. Moreover, we have predicted that the magnetic field curvature does not play any role in the stability of the tearing mode when only passing electrons are considered.

Further analysis has been carried out numerically, by means of linear global gyro-kinetic simulations using GKW code. We have verified our analytic results, namely the linear scaling of the growth rate with $|k'_\parallel|\Delta'$ and the destabilization due to trapped electrons. We have subsequently performed a parametric study of the stability of the tearing mode and we have obtained two main results. First, in the presence of trapped particles, the temperature gradient plays a destabilizing role. Second, we have reported that the magnetic field curvature tends to further destabilize the mode in combination with the temperature gradient, suggesting a destabilization through an interchange mechanism[9]. We have shown that there exists a threshold in temperature gradient below which the magnetic curvature is stabilizing. We have identified a response of trapped particles to the tearing mode which results in a kinetic damping of the mode. The threshold in temperature gradient appears when this kinetic damping is balanced by the interchange destabilization due to the combination of the temperature gradient and the magnetic field curvature. These findings open the way to a deeper understanding of the tearing instability in tokamaks in the presence of kinetic effects and shed light on the dependence of its growth rate on a set of tokamak control parameters.

ACKNOWLEDGMENTS

This work has been carried out thanks to the support of the A*MIDEX project (n° ANR-11-IDEX-0001-02) funded by the «Investissements d'Avenir »French Government program, managed by the French National Research Agency (ANR). This work has been carried out within the framework of the EUROfusion Consortium and French Research Federation for Fusion Studies and has received funding from the Euratom research and training programme 2014-2018 under grant agreement No. 633053. The views and opinions expressed herein do not necessarily reflect those of the European Commission. All the simulations were performed on the MARCONI supercomputer (CINECA) under project reference FUA32_TURBISLE.

Appendix A: Exact linear solution of the gyro-kinetic equation

The starting point to obtain the linear response of electrons is the Vlasov equation in conservative form using a Hamiltonian formalism

$$\frac{\partial F}{\partial t} - [\mathcal{H}, F] = 0 \tag{A1}$$

Here $[X, Y]$ represents the Poisson brackets between X and Y, i.e. $[X, Y] = \partial_{\mathbf{x}} X \partial_{\mathbf{p}} Y - \partial_{\mathbf{p}} X \partial_{\mathbf{x}} Y$, where $\mathbf{x}$ and $\mathbf{p}$ are the position and momenta, forming a set of canonical variables satisfying Hamilton's equations.

The calculation is performed in the so-called δF-approximation. For this purpose we decompose the distribution function and the Hamiltonian into equilibrium and perturbed parts, respectively,

$$F = F_{\text{eq}} + \delta F \tag{A2}$$

$$\mathcal{H} = \mathcal{H}_{\text{eq}} + \delta\mathcal{H} \tag{A3}$$

and assume the gyrokinetic ordering $|\delta F|/F_{\text{eq}} \approx \rho_\star$ and $|\delta\mathcal{H}|/|\mathcal{H}_{\text{eq}}| \approx \rho_\star$. Vlasov equation (A1) for electrons is then linearized and written for δF as

$$\frac{\partial \delta F}{\partial t} - [\mathcal{H}_{\text{eq}}, \delta F] - [\delta\mathcal{H}, F_{\text{eq}}] = 0 \tag{A4}$$

The equilibrium Hamiltonian is given by

$$\mathcal{H}_{\text{eq}} = \frac{|\mathbf{p} - eZ_e\mathbf{A}_{\text{eq}}|^2}{2m_e} + eZ_e\phi_{\text{eq}} \tag{A5}$$

where $\mathbf{A}_{\text{eq}}$ and ϕ_{eq} are respectively the equilibrium vector and electrostatic potentials, $\mathbf{p} = m_e\mathbf{v} + eZ_e\mathbf{A}$ is the electron momentum and Z_e the atomic number of the species, which is $Z_e = -1$ in this particular case where only electrons are considered. The perturbed Hamiltonian is written in terms of the perturbed vector and electrostatic potentials, $A_\parallel$ and ϕ, respectively, as

$$\delta\mathcal{H} = eZ_e\left(\phi - v_{\parallel,\text{eq}}A_\parallel\right) \tag{A6}$$

where $v_{\parallel,\text{eq}}$ is the projection of the electron velocity onto the unperturbed magnetic field lines. This formulation can lead to simple insightful equations of motion when expressed

in canonical variables $(\mathbf{x}, \mathbf{p})$. However, the periodicity of particle motion in a tokamak suggests the use of a different set of canonically conjugated variables, called action-angle variables and represented by $\mathbf{J} = (J_1, J_2, J_3)$ and $\boldsymbol{\alpha} = (\alpha_1, \alpha_2, \alpha_3)$, respectively. These angles describe the gyro-motion (α_1), the motion in the poloidal direction (α_2) and the motion in the toroidal direction (α_3). The equations of motion using these coordinates can be written as

$$\dot{\boldsymbol{\alpha}} = \frac{\partial \mathcal{H}_{\text{eq}}}{\partial \mathbf{J}} = \boldsymbol{\Omega}_{\text{eq}}(\mathbf{J}) \qquad \dot{\mathbf{J}} = -\frac{\partial \mathcal{H}_{\text{eq}}}{\partial \boldsymbol{\alpha}} \tag{A7}$$

where the angles are supposed to vary linearly in time giving the characteristic frequencies of motion at equilibrium $\boldsymbol{\Omega} = (\Omega_1, \Omega_2, \Omega_3)$. For completeness, these frequencies are derived in detail in Appendix C.

We define an equilibrium quantity X_{eq} as the average of the quantity X over the angles $\boldsymbol{\alpha}$, i.e.

$$X_{\text{eq}} \equiv \int \mathrm{d}^3\boldsymbol{\alpha}\, X \tag{A8}$$

which means that the only dependence of X_{eq} is on the actions $\mathbf{J}$, i.e. $X_{\text{eq}} = X_{\text{eq}}(\mathbf{J})$. The equilibrium distribution function and the equilibrium Hamiltonian are therefore functions of the motion invariants and the perturbed distribution function and Hamiltonian are functions of $((\boldsymbol{\alpha}, \mathbf{J}, t)$. Following this definition, the equations of motion A7 introduce the actions as motion invariants, i.e. $\dot{\mathbf{J}} = \mathbf{0}$. Therefore, without any loss of generality, any equilibrium quantity can be defined as a function of the motion invariants associated to the three directions of periodicity.

The periodicity of the perturbed quantities with respect to the angles $\boldsymbol{\alpha}$ allows us to perform a Fourier expansion

$$\begin{Bmatrix} \delta\mathcal{H} \\ \delta F \end{Bmatrix}(\boldsymbol{\alpha}, \mathbf{J}, t) = \sum_{\mathbf{n}\omega} \begin{Bmatrix} \delta\mathcal{H}_{\mathbf{n}\omega} \\ \delta F_{\mathbf{n}\omega} \end{Bmatrix}(\mathbf{J})\ \exp\left[i\left(\mathbf{n}\cdot\boldsymbol{\alpha} - \omega t\right)\right] \tag{A9}$$

where $\mathbf{n} = (n_1, n_2, n_3)$ are the wave numbers associated to the angles $\boldsymbol{\alpha} = (\alpha_1, \alpha_2, \alpha_3)$ and ω is the frequency of the tearing mode. Plugging Eq. (A9) into the linearized Vlasov equation (A4) and using the equations of motion (A7), an exact linear solution can be found

$$\delta F_{\mathbf{n},\omega} = -\frac{\mathbf{n}\cdot\partial_{\mathbf{J}} F_{\text{eq}}}{\omega - \mathbf{n}\cdot\boldsymbol{\Omega}}\, \delta\mathcal{H}_{\mathbf{n},\omega} \tag{A10}$$

In the adiabatic limit, the first motion invariant is proportional to the magnetic moment $\mu = m_e v_\perp / (2B)$, i.e. $J_1 = m_e\mu/(eZ_e)$ and the third motion invariant is the toroidal canonical momentum $J_3 = P_\varphi = -eZ_e\psi + m_e R v_\varphi$, where ψ is the poloidal flux, R is the major radius of the tokamak and v_φ is the projection onto the toroidal direction of the particle velocity. The second motion invariant J_2 does not have a straigthforwardly useable expression for our purpose. Therefore, we perform a change of variable $\mathbf{J} \to \mathbf{I}$, where $\mathbf{I} = (J_1, \mathcal{H}_{\text{eq}}, J_3)$. This change of variable introduces the equilibrium Hamiltonian, i.e. the energy in the absence of any perturbation, which is more convenient for physical analysis. The numerator of Eq. (A10) can therefore be written as follows

$$\mathbf{n}\cdot\partial_{\mathbf{J}} F_{\text{eq}} = \mathbf{n}\cdot\frac{\partial \mathbf{I}}{\partial \mathbf{J}}\cdot\frac{\partial F_{\text{eq}}}{\partial \mathbf{I}} = n_1\frac{\partial F_{\text{eq}}}{\partial J_1} + \mathbf{n}\cdot\boldsymbol{\Omega}\frac{\partial F_{\text{eq}}}{\partial \mathcal{H}_{\text{eq}}} + n_3\frac{\partial F_{\text{eq}}}{\partial J_3} \tag{A11}$$

We can now consider that $\Omega_1 \gg \omega, \Omega_2, \Omega_3$. This ordering yields the exact linear response to be used in the following

$$\delta F_{\mathbf{n},\omega} = \frac{\partial F_{\text{eq}}}{\partial \mathcal{H}_{\text{eq}}}\delta\mathcal{H}_{\mathbf{n},\omega} + \frac{1}{B}\frac{\partial F_{\text{eq}}}{\partial \mu}\delta\mathcal{H}_{\mathbf{n}',\omega} - \frac{\omega\partial_{\mathcal{H}_{\text{eq}}} F_{\text{eq}} + n_3\partial_{J_3} F_{\text{eq}}}{\omega - \mathbf{n}^\star\cdot\boldsymbol{\Omega}}\delta\mathcal{H}_{\mathbf{n}^\star,\omega} \tag{A12}$$

where $\mathbf{n}' = (n_1 \neq 0, n_2, n_3)$ and $\mathbf{n}^\star = (n_1 = 0, n_2, n_3)$.

Appendix B: Perturbed parallel current

The perturbed parallel current is calculated as

$$j_\parallel = eZ_e \int \mathrm{d}^3\mathbf{p}\left(v_{\parallel,\text{eq}}\delta F + \delta v_\parallel F_{\text{eq}}\right) \tag{B1}$$

where the perturbed parallel velocity is expressed in terms of the parallel vector potential

$$\delta v_\parallel = -\frac{eZ_e}{m_e}\delta A_\parallel \tag{B2}$$

Therefore, the perturbed parallel current reads

$$j_\parallel = eZ_e \int \mathrm{d}^3\mathbf{p}\left(v_{\parallel,\text{eq}}\delta F - \frac{eZ_e}{m_e}\delta A_\parallel F_{\text{eq}}\right) \tag{B3}$$

Passing from $(\mathbf{x},\mathbf{p})$ to action-angle variables $(\boldsymbol{\alpha},\mathbf{J})$ at this point requires to pass from a three-dimensional to a six-dimensional space. For this purpose we use the δ-Dirac function such that $j_\parallel$ for electrons is calculated as a 6D integration.

$$j_\parallel(\mathbf{x},t) = eZ_e \int \mathrm{d}^3\mathbf{p}\,\mathrm{d}^3\mathbf{x}'\,\delta\left(\mathbf{x}'-\mathbf{x}\right)\left(v_{\parallel,\mathrm{eq}}\delta F - \frac{eZ_e}{m_e}\delta A_\parallel F_{\mathrm{eq}}\right) \tag{B4}$$

where $\mathbf{x}'$ is a spatial position for the integration. We can now make the canonical change of variable $(\mathbf{x},\mathbf{p}) \to (\boldsymbol{\alpha},\mathbf{J})$ which gives

$$j_\parallel(\mathbf{x},t) = eZ_e \int \mathrm{d}\tau^\star\,\mathrm{d}\alpha_1\delta(\mathbf{x}'-\mathbf{x})\left(v_{\parallel,\mathrm{eq}}\delta F - \frac{eZ_e}{m_e}\delta A_\parallel F_{\mathrm{eq}}\right) \tag{B5}$$

where we have separated the integration variables into gyrophase $\mathrm{d}\alpha_1 \equiv \mathrm{d}\varphi_c$ and $\mathrm{d}\tau^\star = \mathrm{d}\alpha_2\,\mathrm{d}\alpha_3\,\mathrm{d}J_1\,\mathrm{d}J_2\,\mathrm{d}J_3$. We make use of Parseval's identity for Fourier series,

$$\int \frac{\mathrm{d}\alpha_1}{2\pi}\delta(\mathbf{x}'-\mathbf{x})\delta F = \sum_{n_1}\left[\delta(\mathbf{x}'-\mathbf{x})\right]_{n_1}\delta F^\dagger_{n_1} \tag{B6}$$

where the $\dagger$ designates the complex conjugate of the perturbed quantity. The n_1 mode of the Dirac function can be calculated using the definition of the Dirac distribution

$$\begin{aligned}\left[\delta(\mathbf{x}'-\mathbf{x})\right]_{n_1} &= \int \frac{d\alpha_1}{2\pi}\delta(\mathbf{x}'-\mathbf{x})\,\mathrm{e}^{-in_1\alpha_1} \\ &= \int\frac{d\alpha_1}{2\pi}\int\frac{d^3\,\mathbf{k}}{(2\pi)^3}\;\mathrm{e}^{i\mathbf{k}\cdot\mathbf{x}'-i\mathbf{k}\cdot\mathbf{x}}\,\mathrm{e}^{-in_1\alpha_1}\end{aligned} \tag{B7}$$

Therefore, the parallel current density in Eq. (B5) can be expressed using the Bessel function of the first kind, defined as $\int d\alpha_1/(2\pi)\,\mathrm{e}^{i(k_\perp\rho_c\cos\alpha_1-n_1\alpha_1)} = (-i)^{n_1}J_{n_1}(k_\perp\rho_c)$

$$j_\parallel(\mathbf{x},t) = eZ_e\int \mathrm{d}\tau^\star\sum_{n_1}(-i)^{n_1}\int\frac{\mathrm{d}^3\mathbf{k}}{(2\pi)^3}\,\mathrm{e}^{i\mathbf{k}\cdot(\mathbf{x}_G-\mathbf{x})}J_{n_1}(k_\perp\rho_c)\left(v_{\parallel,\mathrm{eq}}\delta F^\dagger_{n_1} - \frac{eZ_e}{m_e}\delta A^\dagger_{\parallel n_1}F_{\mathrm{eq}}\right) \tag{B8}$$

Here the perturbed quantities are functions of $(\mathbf{x}_G,\mathcal{H}_{\mathrm{eq}},P_\varphi)$. Note that through this Hamiltonian formalism one can obtain the parallel current associated to the particle motion, in terms of particle coordinates $\mathbf{x}$, using physical quantities describing the guiding-center motion, which depend on guiding-center coordinates $\mathbf{x}_G$. Similarly, we calculate the n_1-mode of each component of δF and we plug it into the expression of the parallel current in Eq. (B8). Anticipating the fact that we will later use the deeply passing particle approximations, we pass to an integration in guiding center coordinates $\mathrm{d}\tau^\star = \mathrm{d}\alpha_2\,\mathrm{d}\alpha_3\,\mathrm{d}J_1\,\mathrm{d}J_2\,\mathrm{d}J_3 \to \mathcal{J}\,\mathrm{d}\mathbf{x}_G\,\mathrm{d}v_{\parallel,\mathrm{eq}}v_\perp\,\mathrm{d}v_\perp$, where $\mathcal{J}$ is the Jacobian of the transformation. We now make use again of the ordering $\Omega_1 \gg \omega,\Omega_2,\Omega_3$, which implies that the third term in the right-hand side of Eq. (4) is negligible except for $n_1 = 0$. Therefore, we keep only the $n_1 = 0$ terms, which strictly speaking is the exactly the same as performing a gyro-average. Using the Bessel function property $\sum_{n=-\infty}^{+\infty}J_n^2(x) = 1$[5] and the inverse Fourier transform

$$\int\frac{\mathrm{d}^3\mathbf{k}}{(2\pi)^3}\,\delta\hat{\mathcal{H}}^\dagger(\mathbf{k},t)\;\mathrm{e}^{-i\mathbf{k}\cdot\mathbf{x}} = \delta\mathcal{H}(\mathbf{x},t) \tag{B9}$$

we obtain the following general expression for the parallel current in the gyro-kinetic approach using the magnetic limit, i.e. neglecting the electrostatic potential

$$\begin{aligned} j_\parallel(\mathbf{x},t) = &-e^2\int\mathcal{J}\,\mathrm{d}v_{\parallel,\mathrm{eq}}\,\mathrm{d}\mu\left\{v^2_{\parallel,\mathrm{eq}}\partial_{\mathcal{H}_{\mathrm{eq}}}F_{\mathrm{eq}}\delta A_\parallel(\mathbf{x},t)\right. \\ &+ v^2_{\parallel,\mathrm{eq}}\frac{1}{B}\frac{\partial F_{\mathrm{eq}}}{\partial\mu}\left(1-J_0^2\right)\delta A_\parallel(\mathbf{x},t) \\ &+\sum_{n_2,n_3}v^2_{\parallel,\mathrm{eq}}\frac{\omega\partial_{\mathcal{H}_{\mathrm{eq}}}F_{\mathrm{eq}}+n_3\partial_{J_3}F_{\mathrm{eq}}}{\omega-n_2\Omega_2-n_3\Omega_3}J_0^2\delta A_{\parallel n_2,n_3,\omega}(\mathbf{x}) \\ &\times\mathrm{e}^{i(n_2\alpha_2+n_3\alpha_3-\omega t)} \\ &\left.+\frac{1}{m_e}F_{\mathrm{eq}}\delta A_\parallel(\mathbf{x},t)\right\} \end{aligned} \tag{B10}$$

where $J_0 \equiv J_0(k_\perp\rho_c)$, J_0^2 represents the gyro-average operator applied twice and the squared electron charge $Z_e^2 = 1$ has been removed for the sake of clarity. We choose the equilibrium distribution function

$$F_{\mathrm{eq}} = \frac{n_{\mathrm{eq}}}{\left(2\pi T_{\mathrm{eq}}/m_e\right)^{3/2}}\,\mathrm{e}^{-\frac{\mathcal{H}_{\mathrm{eq}}}{T_{\mathrm{eq}}}} \tag{B11}$$

where n_{eq} and T_{eq} are the equilibrium density and temperature, respectively. After integrating the first and last terms of the right-hand side in expression (B10), they cancel out. The second term with the $\partial F_{\mathrm{eq}}/\partial\mu$ vanishes as F_{eq} does not explicitly depend on the magnetic moment. For electrons, one can take the small orbit limit and approximate the Bessel function as $J_0^2(k_\perp\rho_c) \approx 1$ for $k_\perp\rho_c \ll 1$. Finally, $j_\parallel(\mathbf{x},t)$ is written as

$$j_{\parallel}\left(\mathbf{x},t\right)=\frac{e^{2}}{T_{\mathrm{eq}}}\sum_{n_{2},n_{3}}\left\langle v_{\parallel,\mathrm{eq}}^{2}\frac{\omega-n_{3}T_{\mathrm{eq}}\partial_{J_{3}}\log F_{\mathrm{eq}}}{\omega-n_{2}\Omega_{2}-n_{3}\Omega_{3}}\right\rangle \delta A_{\parallel n_{2},n_{3},\omega}\left(\mathbf{x}\right)\,\mathrm{e}^{i(n_{2}\alpha_{2}+n_{3}\alpha_{3}-\omega t)} \tag{B12}$$

where the notation $\langle\cdots\rangle$ has been used for simplicity to represent an average over gyro-centre equilibrium velocity space weighted by the equilibrium distribution function

$$\langle\cdots\rangle=\int\mathcal{J}\,\mathrm{d}v_{\parallel,\mathrm{eq}}\,\mathrm{d}\mu\,\cdots\,F_{\mathrm{eq}} \tag{B13}$$

If we restrict our analysis to deeply passing electrons, we can write $\alpha_2=\theta$ and $\alpha_3=\varphi$, where θ and φ are the poloidal and toroidal angles, respectively. Consequently $n_2=m$ and $n_3=n$, with m and n the poloidal and toroidal mode numbers, respectively. The frequencies Ω_2 and Ω_3 are calculated in detail in Appendix C. For deeply passing particles, these frequencies can be approximated as

$$\Omega_{2}\approx\frac{v_{\parallel,\mathrm{eq}}}{qR_{0}} \tag{B14}$$

$$\Omega_{3}\approx\frac{2q}{r}\frac{m_{e}v_{\parallel,\mathrm{eq}}^{2}+\mu B_{0}}{eZ_{e}B_{0}R_{0}}+\frac{v_{\parallel,\mathrm{eq}}}{R_{0}} \tag{B15}$$

where q is the safety factor, which represents the helicity of the magnetic field lines, and r is the minor radius. B_0 and R_0 are respectively, the modulus of the magnetic field and the major radius, measured at the magnetic axis. The perturbed parallel current will be written in normalized units. For this purpose we normalize the velocities to the thermal velocity of electrons v_{th}, the distances to R_0, the frequencies to the transit frequency $\omega_t=v_{\mathrm{th}}/R_0$, the equilibrium distribution function to n_0/v_{th}^3, with n_0 some normalizing density, the parallel vector potential to $B_0R_0\rho_\star^2$ and the temperature to a normalizing temperature defined as $T_0=m_ev_{\mathrm{th}}^2/2$. The parallel current can then be rewritten as

$$j_{\parallel}\left(\mathbf{x},t\right)=\rho_{\star}en_{0}v_{\mathrm{th}}\frac{2}{\hat{T}_{\mathrm{eq}}}\sum_{m,n,\omega}\left\langle \hat{v}_{\parallel}^{2}\frac{\hat{\omega}-\hat{\omega}_{\star g}}{\hat{\omega}-\hat{k}_{\parallel}\hat{v}_{\parallel}-\hat{\omega}_{D}}\right\rangle \delta\hat{A}_{\parallel m,n,\omega}\left(\mathbf{x}\right)\,\mathrm{e}^{i(m\theta+n\varphi-\omega t)} \tag{B16}$$

with $\hat{\cdot}$ representing normalized quantities. The parallel wave vector $k_\parallel$ is given by $k_\parallel=\left(m/q-n\right)/R_0$ and the magnetic drift frequency ω_D is given by $\omega_D=2qn/r\left(m_ev_{\parallel,\mathrm{eq}}^2+\mu B_0\right)/\left(eZ_eB_0R_0\right)$. Notice that $k_\parallel$ vanishes on the rational surface defined as $q=m/n$. In the remainder of this paper, the *eq* subscript for the parallel velocity will be dropped for the sake of simplicity. Note that $\rho_\star$ gives the typical ordering between the equilibrium and the perturbed distribution function and en_0v_{th} is the normalization for the current. In this expression we have introduced the generalized diamagnetic frequency $\omega_{\star g}=nT_{\mathrm{eq}}\partial_{J_3}\log F_{\mathrm{eq}}$, which includes all the spatial dependence of the equilibrium. For thermal particles, at lowest order in $\rho_\star$, one can write $J_3\approx-eZ_e\psi$. Therefore, the derivative with respect to J_3 can be reduced to a derivative with respect to the radial position.

Appendix C: Equilibrium frequencies of motion

The motion of a charged particle in toroidal geometry can be divided into a parallel and a drift motion (at lower order), $\mathbf{v}=v_\parallel\mathbf{b}+\mathbf{v_g}$, in which we omit the $\mathbf{E}\times\mathbf{B}$ drift. Note that this term can be added, however one needs to be careful that it is independent of the toroidal motion so that the toroidal momentum can still be a motion invariant. The time evolution of the motion can be given by,

$$\dot{\Psi}=\mathbf{v}.\nabla\Psi \tag{C1}$$

$$\dot{\theta}=v_\parallel\mathbf{b}.\nabla\theta+\mathbf{v_g}.\nabla\theta \tag{C2}$$

$$\dot{\varphi}=v_\parallel q\,\mathbf{b}.\nabla\theta+\mathbf{v_g}.\nabla\varphi \tag{C3}$$

where Psi is the poloidal flux, θ and φ are the poloidal and toroidal coordinates, respectively. The magnetic drift velocity $\mathbf{v_g}$ is given by,

$$\mathbf{v_g}=\frac{mv_\parallel^2+\mu B_0}{eB_0}\left(\mathbf{b_0}\times\frac{\nabla B_0}{B_0}\right) \tag{C4}$$

The energy is defined as

$$E=\frac{1}{2}mv_\parallel^2+\mu B_0(\theta) \tag{C5}$$

so that equation (C2) is expressed at lowest order in $\rho_\star$, the Larmor radius normalized to the Tokamak major radius, as

follows

$$\dot{\theta} = \epsilon_{\parallel}\sqrt{2/m}\,[E-\mu B_0(\theta)]^{1/2}\,\frac{\mathbf{B_0}\cdot\nabla\theta}{B_0} \tag{C6}$$

$\epsilon_{\parallel}$ designates the sign of the parallel velocity. We define the helical angle as $\zeta = \varphi - q\theta$. The time derivative of ζ gives,

$$\dot{\zeta} = \dot{\varphi} - q(\bar{\Psi})\dot{\theta} \tag{C7}$$

where $\bar{\Psi}$ is the flux surface at the resonance layer. Using eq. (C2) and the fact that $q(\Psi) - q(\bar{\Psi}) = (dq/dr)\delta\Psi$, we get,

$$\dot{\zeta} = \frac{dq}{d\Psi}\delta\Psi\dot{\theta} + \mathbf{v_g}\cdot\nabla\zeta \tag{C8}$$

It follows that the three angular motions are found to be the gyromotion, the poloidal motion and the toroidal motion (also called, respectively, the bounce and precessional motions, for trapped particles). Their respective frequencies are written as,

$$\Omega_1 = \Omega_b\oint\frac{d\theta}{2\pi}\frac{1}{\dot{\theta}}\dot{\gamma} \approx \Omega_b\oint\frac{d\theta}{2\pi}\frac{1}{\dot{\theta}}\frac{eB_0}{m} \tag{C9}$$

$$\Omega_2 = \Omega_b \approx 2\pi\left(\oint\frac{d\theta}{\dot{\theta}}\right)^{-1} \tag{C10}$$

$$\Omega_3 = \Omega_b\oint\frac{d\theta}{2\pi}\frac{1}{\dot{\theta}}\dot{\varphi} \approx \Omega_b\oint\frac{d\theta}{2\pi}\frac{1}{\dot{\theta}}\mathbf{v_D}\cdot\big[-q'(\bar{\Psi})\theta\nabla\Psi + \nabla\left((\varphi - q(\bar{\Psi})\theta)\right)\big] + q(\bar{\Psi})\Omega_b\oint\frac{d\theta}{2\pi} \tag{C11}$$

Note that for passing particles, $\oint = \int_{-\pi}^{+\pi}$ whereas for trapped particles oscillating on $[-\theta_0, \theta_0]$,$\oint = \int_{-\theta_0}^{+\theta_0}$.

1. The poloidal frequency Ω_2

At the lowest order, the parallel velocity dominates the drift velocity, and the bounce frequency can be rewritten as,

$$\Omega_2^{-1} = \oint\frac{d\theta}{2\pi}\frac{1}{\mathbf{b}\cdot\nabla\theta v_{\parallel}} \tag{C12}$$

We consider a simple circular equilibrium, with a large aspect ratio where the equilibrium magnetic field is given by

$$\mathbf{B_0} = \nabla\Psi\times\nabla\zeta \tag{C13}$$

Here $\zeta = \varphi - q(\Psi)\theta$ is the binormal coordinate. In this geometry, the magnitude of the equilibrium magnetic field can be expressed to the first order as $B_{(0)} = B_0(1-\epsilon\cos\theta)$ and $\mathbf{b}\cdot\nabla\theta \approx 1/qR$. It comes,

$$\Omega_2^{-1} = \oint\frac{\mathrm{d}\theta}{2\pi}\frac{qR}{v_{\parallel}} \tag{C14}$$

To the first order in $\epsilon = r/R_0$, the major radius is expressed

$$R = R_0\,(1+\epsilon\cos\theta) \tag{C15}$$

Expressing the parallel velocity in terms of the energy defined in Eq. (C5)

$$v_{\parallel} = \sqrt{2(E-\mu B_{(0)})/m} = \sqrt{\frac{2E}{m}}\sqrt{1-\frac{\mu B_{(0)}}{E}} \tag{C16}$$

one can write Eq. (C14) as

$$\Omega_2^{-1} = \epsilon_{\parallel}qR_0\sqrt{\frac{m}{2E}}\,\bar{\Omega}_b^{-1} \tag{C17}$$

Where $\bar{\Omega}_b^{-1}$ is the integral given as a first order in ϵ by

$$\bar{\Omega}_b^{-1} = \oint\frac{d\theta}{2\pi}\frac{1}{\sqrt{1-\lambda(1-\epsilon\cos\theta)}} \tag{C18}$$

with $\lambda = \mu B_0/E$. Keeping the first order effects in ϵ, we define a parameter κ which differentiates the trapping and passing domains

$$\kappa^2 = \frac{2\epsilon\lambda}{1-(1-\epsilon)\lambda} \tag{C19}$$

and we rewrite Eq. (C18) as

$$\bar{\Omega}_b^{-1} = \frac{\kappa}{\sqrt{2\epsilon\lambda}}\oint\frac{d\theta}{2\pi}\frac{1}{\sqrt{1-\kappa^2\sin^2(\theta/2)}} \tag{C20}$$

The integral (C20) is to be solved separately for passing and trapped particles by integrating over the appropriate boundaries

$$\text{for passing particles}(\kappa<1):\ \theta_1 = -\pi,\ \theta_2 = +\pi \tag{C21}$$

$$\text{for trapped particles}(\kappa>1):\ \theta_1 = -\theta_0,\ \theta_2 = +\theta_0 \tag{C22}$$

Consequently, an appropriate change of variables is made for treating each class of particles. For passing particles, we make the change of variable $u = \theta/2$, and for trapped particles $\sin u = \kappa\sin(\theta/2)$ such that $0 \le u \le \pi/2$ and $0 \le \theta \le \theta_0$. The integral (C20) is then expressed in terms of the elliptic integral of the first kind $\mathbb{K}(m)$ as defined in Ref. 5,

$$\mathbb{K}(\mathrm{m}) = \int_0^{\pi/2}\mathrm{d}\theta\frac{1}{\sqrt{1-\mathrm{m}\sin^2\theta}} \tag{C23}$$

It finally comes that

$$\bar{\Omega}_b^{-1} = \frac{\kappa}{\sqrt{2\epsilon\lambda}}\frac{2}{\pi}\begin{cases}\mathbb{K}(\kappa^2) & \text{for passing particles}\\ \frac{1}{\kappa}\,\mathbb{K}(1/\kappa^2) & \text{for trapped particles}\end{cases} \tag{C24}$$

Finally, the poloidal frequency Ω_2 is calculated for passing and trapped particles, locally, in circular geometry to the leading order in ϵ and it is expressed as

$$\Omega_2 = \epsilon_{\parallel}\frac{q}{R_0}\sqrt{\frac{2E}{m}}\,\frac{\sqrt{2\epsilon\lambda}}{\kappa}\,\frac{\pi}{2}\begin{cases}\mathbb{K}^{-1}(\kappa^2) & \text{for passing}\\ \kappa\,\mathbb{K}^{-1}(1/\kappa^2) & \text{for trapped}\end{cases} \tag{C25}$$

2. The toroidal frequency Ω_3

The precessional frequency is given to the first order in ϵ by

$$\Omega_3 = \bar{\Omega}_b \oint \frac{d\theta}{2\pi} \frac{\mu B_{(0)} + m v_\parallel^2}{\sqrt{1-\lambda(1-\epsilon\cos\theta)}} \frac{\mathbf{B_{(0)}} \times \nabla B_{(0)}}{e B_{(0)}^3} \cdot \cdot \left[-\frac{dq}{d\Psi} s\theta \nabla\Psi + \nabla\zeta \right] + q(\bar{\Psi})\Omega_b \oint \frac{d\theta}{2\pi} \quad \text{(C26)}$$

In order to evaluate the integral in Eq. (C26), we explicit the projection of the curvature term onto $\nabla\Psi$ and $\nabla\zeta$ using Eq. (C13)

$$\begin{aligned} (\mathbf{B_0} \times \nabla B_0).\nabla\Psi &= -\nabla B_0 \cdot (\nabla\Psi \times \nabla B_0) \\ &= -\nabla B_0 \cdot [\nabla\Psi \times (\nabla\Psi \times \nabla\zeta)] \quad \text{(C27)} \\ &= -|\nabla\Psi|^2 |\nabla\zeta|^2 (\partial B_0/\partial\zeta) \\ (\mathbf{B_0} \times \nabla B_0).\nabla\zeta &= \nabla B_0 \cdot (\nabla\zeta \times \nabla B_0) \\ &= -\nabla B_0 \cdot [\nabla\zeta \times (\nabla\Psi \times \nabla\zeta)] \quad \text{(C28)} \\ &= -|\nabla\zeta|^2 |\nabla\Psi|^2 (\partial B_0/\partial\Psi) \end{aligned}$$

Writing $\mu B_0 + m v_\parallel^2 = 2E - \mu B_0$, the expression of the toroidal frequency Ω_3 becomes,

$$\Omega_3 = \bar{\Omega}_b \frac{E B_0}{e R_0 B_0^3} |\nabla\zeta|^2 |\nabla\Psi| \oint \frac{d\theta}{2\pi} \frac{(2-\lambda)(s\theta\sin\theta + \cos\theta)}{\sqrt{1-\lambda(1-\epsilon\cos\theta)}} + \delta_{passing} q(r)\Omega_2 \quad \text{(C29)}$$

Since $\mathrm{d}\Psi/\mathrm{d}r = B_0 r/q$ and $|\nabla\zeta| \approx q/r$, it follows that Eq. (C29) is written

$$\Omega_3 = \frac{q}{r} \frac{E}{e B_0 R_0} \bar{\Omega}_d + \delta_{passing} q(r)\Omega_2 \quad \text{(C30)}$$

Where $\bar{\Omega}_d$ is given in terms of Ω_2 given by Eq. (C25)

$$\bar{\Omega}_d = \bar{\Omega}_b (2-\lambda)\Omega_\kappa \quad \text{(C31)}$$

With $2-\lambda = \frac{4\epsilon+\kappa^2(1-2\epsilon)}{2\epsilon+(1-\epsilon)\kappa^2}$ and Ω_κ is the integral given by

$$\Omega_\kappa = \int_{\theta_1}^{\theta_2} \frac{d\theta}{2\pi} \frac{(s\theta\sin\theta + \cos\theta)}{\sqrt{1-\lambda(1-\epsilon\cos\theta)}} \quad \text{(C32)}$$

The integral (C32) is also solved separately for passing and trapped particles by integrating over the appropriate boundaries given in Eqs. (C21) and (C22). For the $\cos\theta$ integral, we notice that $\cos\theta = 1 - \sin^2\frac{\theta}{2}$, so the convenient change of variable would be $u = \theta/2$ for passing particles and $\sin u = \sin\theta/2$ for trapped particles. As for the $\sin\theta$ integral, we solve it integrating by parts as we notice that

$$\frac{\mathrm{d}}{\mathrm{d}\theta}\left(\sqrt{1-\kappa^2\sin^2\frac{\theta}{2}}\right) = -\frac{\kappa^2}{2}\frac{\sin\theta}{2\sqrt{1-\kappa^2\sin^2\frac{\theta}{2}}} \quad \text{(C33)}$$

Therefore,

$$\int_{\theta_1}^{\theta_2} \frac{\mathrm{d}\theta}{2\pi} \frac{\theta\sin\theta}{\sqrt{1-\kappa^2\sin^2\frac{\theta}{2}}} = -\frac{4}{\kappa^2}\left[\frac{\theta}{2\pi}\sqrt{1-\kappa^2\sin^2\left(\frac{\theta}{2}\right)}\right]_{\theta_1}^{\theta_2} + \frac{4}{\kappa^2}\int_{\theta_1}^{\theta_2}\frac{\mathrm{d}\theta}{2\pi}\sqrt{1-\kappa^2\sin^2\left(\frac{\theta}{2}\right)} \quad \text{(C34)}$$

The term between brackets is equal to zero for trapped particles, as $\kappa^2\sin^2(\theta/2) = 1$. However, for passing particles, $\theta_1 = -\pi$ and $\theta_2 = +\pi$, it does not vanish and it gives $\sqrt{1-\kappa^2}$. Using the standard definition of the complete elliptic integrals of the first kind given by (C23) and that of the second kind given by[5],

$$\mathbb{E}(\mathrm{m}) = \int_0^{\pi/2} \mathrm{d}\theta \sqrt{1-\mathrm{m}\sin^2\theta} \quad \text{(C35)}$$

Finally, $\bar{\Omega}_d$ can be expressed as

$$\bar{\Omega}_d = \begin{cases} \frac{4\epsilon+\kappa^2(1-2\epsilon)}{2\epsilon+(1-\epsilon)\kappa^2}\left[1 + \frac{2}{\kappa^2}\left(\frac{\mathbb{E}(\kappa^2)}{\mathbb{K}(\kappa^2)} - 1\right) + \frac{4s}{\kappa^2}\left(\frac{\mathbb{E}(\kappa^2)}{\mathbb{K}(\kappa^2)} - \frac{\pi}{2}\frac{\sqrt{1-\kappa^2}}{\mathbb{K}(\kappa^2)}\right)\right] & \text{for passing particles } (\kappa < 1) \\ \frac{4\epsilon+\kappa^2(1-2\epsilon)}{2\epsilon+(1-\epsilon)\kappa^2}\left[2\frac{\mathbb{K}(1/\kappa^2)}{\mathbb{E}(1/\kappa^2)} - 1 + 4s\left(\frac{\mathbb{K}(1/\kappa^2)}{\mathbb{E}(1/\kappa^2)} + \frac{1}{\kappa^2} - 1\right)\right] & \text{for trapped particles } (\kappa > 1) \end{cases} \quad \text{(C36)}$$

Appendix D: Impact of the magnetic field curvature on the tearing instability through mode-mode coupling

In all the previous sections, we have considered a single harmonic for the perturbation, thus neglecting possible couplings between the different harmonics. However multiple rational surfaces may be present within the domain and so allows double tearing modes and toroidal coupling of modes, a process which is known to be destabilizing[11]. We have neglected also the electrostatic potential and treated the in-

stability in a purely magnetic approach. Of course, although they can be insightful, these approximations make our model less accurate as we neglect some physical mechanisms that are important in understanding the role of magnetic curvature. For this reason, we investigate in this section the effect of curvature through toroidal coupling of main resonating mode, which we consider here as the principal harmonic, and one of its side bands. The electrostatic potential is considered here. However, Poisson equation is not solved because we use the ideal MHD condition outside of the resonant surface to to relate $\widetilde{\phi}$ to $\widetilde{A}_\parallel$. We start with the electromagnetic drift kinetic equation that describes the electron dynamics. The perturbed distribution function δF is decomposed into adiabatic and non adiabatic parts

$$\delta F = \frac{e}{T_e} F_{\rm eq}\phi + g \tag{D1}$$

where $F_{\rm eq}$ is the background distribution, considered as a Maxwellian, and g is the non adiabatic distribution function, satisfying the equation

$$(\omega - k_\parallel v_\parallel - \omega_D) g = -(\omega - \omega_{\star n})\frac{eF_{\rm eq}}{T_e}\left(\phi - \frac{v_\parallel}{c}A_\parallel\right) \tag{D2}$$

where ϕ and $A_\parallel$ are the perturbed electrostatic potential and the parallel component of the magnetic vector potential, respectively. In this equation, the magnetic drift frequency is expressed as a differential operator

$$\omega_D = -i\,\mathbf{v_D}\cdot\nabla = \frac{v_\parallel^2 + \mu B}{eB_0R_0}\left(\sin\theta\frac{\partial}{\partial r} + \cos\theta\frac{\partial g}{r\partial\theta}\right) \tag{D3}$$

r and θ are respectively the radial coordinate and the poloidal angle. We consider the toroidal coupling of modes m and $m+1$, where m is the poloidal wave number. Perturbations are then expressed in the form

$$Q = Q_m\,\mathrm{e}^{im\theta} + Q_{m+1}e^{i(m+1)\theta} \tag{D4}$$

Assuming $\partial_r g_m = \partial_r g_{m+1} = 0$ and separating the main oscillating component from the side band, the Vlasov equation is rewritten as

$$\mathcal{M}\begin{pmatrix} g_m \\ g_{m+1}\end{pmatrix} = S\begin{pmatrix} \phi_m - v_\parallel A_{\parallel m} \\ \phi_{m+1} - v_\parallel A_{\parallel m+1}\end{pmatrix} \tag{D5}$$

where the matrix $\mathcal{M}$ is the square matrix

$$\mathcal{M} = \begin{pmatrix} \omega - k_{\parallel m}v_\parallel & \frac{i(m+1)}{2r}v_D \\ \frac{im}{2r}v_D & \omega - k_{\parallel m+1}v_\parallel\end{pmatrix} \tag{D6}$$

$S = -(\omega - \omega_{\star n})eF_{\rm eq}/T_e$ and $v_D = (v_\parallel^2 + \mu B)/eB_0R_0$, B_0 is the equilibrium magnetic field. The parallel wave vector $k_\parallel$ takes a different form depending on the considered poloidal mode such that $k_{\parallel m} = (m/q_m + n)/R$ is evaluated at the resonant surface r_m and $k_{\parallel m+1} = ((m+1)/q_{m+1} + n)/R$ at the resonant surface r_{m+1}. The solution of Eq. (D6) can be obtained by inverting the matrix $\mathcal{M}$,

$$\mathcal{M}^{-1} = \frac{1}{|\mathcal{M}|}\begin{pmatrix} \omega - k_{\parallel m+1}v_\parallel & -\frac{i(m+1)}{2r}v_D \\ -\frac{im}{2r}v_D & \omega - k_{\parallel m}v_\parallel\end{pmatrix} \tag{D7}$$

where $|\mathcal{M}| = \det(\mathcal{M}) = (\omega - k_{\parallel m}v_\parallel)(\omega - k_{\parallel m+1}v_\parallel) + v_D^2 m(m+1)/4r^2$ is the determinant of matrix $\mathcal{M}$. The dispersion relation of the tearing mode is obtained by integrating Ampère's law for each mode. In the constant-ψ approximation, this reads in normalized units

$$\delta_e^2\,\Delta'_m A_{\parallel m} = \frac{4}{\sqrt{\pi}}\int_{\mathbb{R}}\mathrm{d}x\int \mathrm{d}v_\parallel v_\perp dv_\perp v_\parallel\, g_m \tag{D8}$$

$$\delta_e^2\,\Delta'_{m+1} A_{\parallel m+1} = \frac{4}{\sqrt{\pi}}\int_{\mathbb{R}}\mathrm{d}x\int \mathrm{d}v_\parallel v_\perp\,\mathrm{d}v_\perp v_\parallel\, g_{m+1} \tag{D9}$$

In matrix form this system of equations can be written as

$$\begin{pmatrix}\Delta'_m & 0 \\ 0 & \Delta'_{m+1}\end{pmatrix}\begin{pmatrix} A_{\parallel m} \\ A_{\parallel m+1}\end{pmatrix} = \mathcal{I}\begin{pmatrix} A_{\parallel m} \\ A_{\parallel m+1}\end{pmatrix} \tag{D10}$$

where $\mathcal{I}$ is a matrix that will be calculated in the following. The perturbed distribution functions associated to modes m and $m+1$, respectively at the resonant surfaces r_m and r_{m+1} are expressed as

$$g_m = -\frac{(\omega - k_{\parallel m+1}v_\parallel)(\phi_m - v_\parallel A_{\parallel m}) - i\frac{m+1}{2r}v_D(\phi_{m+1} - v_\parallel A_{\parallel m+1})}{(\omega - k_{\parallel m}v_\parallel)(\omega - k_{\parallel m+1}v_\parallel) + \frac{m(m+1)}{4r^2}v_D^2}(\omega - \omega_{\star n})e^{-v_\parallel^2 - v_\perp^2} \tag{D11}$$

$$g_{m+1} = -\frac{-i\frac{m}{2r}v_D(\phi_m - v_\parallel A_{\parallel m}) + (\omega - k_{\parallel m}v_\parallel)(\phi_{m+1} - v_\parallel A_{\parallel m+1})}{(\omega - k_{\parallel m}v_\parallel)(\omega - k_{\parallel m+1}v_\parallel) + \frac{m(m+1)}{4r^2}v_D^2}(\omega - \omega_{\star n})e^{-v_\parallel^2 - v_\perp^2} \tag{D12}$$

Therefore, the response of mode m is given by the combination of the modes m and $m+1$ of the potential. The same can be said about the mode $m+1$. The integrals in Eqs.

(D8) (first line of matrix $\mathcal{I}$) and (D9) (second line of matrix $\mathcal{I}$) are respectively calculated around the resonant surfaces r_m and r_{m+1}.

The resonant condition $\omega - k_\parallel v_\parallel$ at one of the resonant surfaces can be simplified when evaluated at the other surface. In fact, away from the resonant surface r_m, the parallel streaming motion is much faster that the frequency of the mode, however close to that surface, the resonance is satisfied and one can write $\omega - k_{\parallel m} v_\parallel \approx 0$. This allows to write

$$(\omega - k_{\parallel m+1} v_\parallel)\big|_{r_m} = \omega - \frac{1}{R_0}\left(\frac{m+1}{q_{m+1}} + n\right)\Big|_{r_m} v_\parallel = \omega - k_{\parallel m} v_\parallel - \frac{v_\parallel}{q_{m+1} R_0} \approx -\frac{v_\parallel}{q_{m+1} R_0} \tag{D13}$$

$$(\omega - k_{\parallel m} v_\parallel)\big|_{r_{m+1}} = \omega - \frac{1}{R_0}\left(\frac{m}{q_m} + n\right)\Big|_{r_{m+1}} v_\parallel = \omega - k_{\parallel m+1} v_\parallel - \frac{v_\parallel}{q_m R_0} \approx \frac{v_\parallel}{q_m R_0} \tag{D14}$$

We assume that the magnetic drift is constant on each of the resonant surfaces (the local approximation). Inside the resonant layer, we consider that the corresponding electrostatic potential is equal to zero. And outside of it, the ideal MHD condition applies i.e. the parallel electric field vanishes at that position. Therefore, on the resonance surface r_m, $E_{\parallel m+1} = 0$, i.e $\phi_{m+1} = \omega A_{\parallel m+1} k_{\parallel m+1}$ and on $r_m + 1$; $E_{\parallel m} = 0$, i.e. $\phi_m = \omega A_{\parallel m} k_{\parallel m}$. On these grounds, we calculate each term of matrix $\mathcal{I}$ of Eq. (D10)

$$\mathcal{I}_{m,m} \approx -\frac{\omega_{pe}^2}{c^2}\frac{4}{\sqrt{\pi}} \int \mathrm{d}v_\parallel v_\perp \, \mathrm{d}v_\perp \frac{v_\parallel^3}{R q_{m+1}} (\omega - \omega_{\star n}) e^{-v_\parallel^2 - v_\perp^2} \frac{R q_{m+1}}{v_\parallel} \int \mathrm{d}x \frac{1}{k'_{\parallel m} x v_\parallel - \omega + \frac{m(m+1) v_D^2 R q_{m+1}}{4 r_m^2 v_\parallel}} \tag{D15}$$

$$\begin{aligned}\mathcal{I}_{m,m+1} = &-\frac{4}{\sqrt{\pi}} i \int \mathrm{d}v_\parallel v_\perp \, \mathrm{d}v_\perp (\omega - \omega_{\star n}) e^{-v_\parallel^2 - v_\perp^2} R q_{m+1} \frac{m+1}{2 r_m} v_D \\ &\left\{ \int \mathrm{d}x \frac{\omega}{k'_{\parallel m+1} k'_{\parallel m} v_\parallel x^2 - \omega k'_{\parallel m+1} x + \frac{m(m+1) v_D^2 R q_{m+1}}{4 r_m^2 v_\parallel} k'_{\parallel m+1} x} + v_\parallel \int \mathrm{d}x \frac{1}{k'_{\parallel m} x v_\parallel - \omega + \frac{m(m+1) v_D^2 R q_{m+1}}{4 r_m^2}} \right\}\end{aligned} \tag{D16}$$

After integration over x and $v_\perp$ and using the definition of the complex logarithm, the matrix elements $\mathcal{I}_{m,m}$ and $\mathcal{I}_{m,m+1}$ become $\mathcal{I}_{m,m} = -i \frac{2\sqrt{\pi}}{|k'_{\parallel m}|} \left[\omega - \hat{\omega}_{\star e}(1 + \frac{1}{2}\eta_e)\right]$ and $\mathcal{I}_{m,m} = 0$.

We perform the same calculation for $\mathcal{I}_{m+1,m}$ and $\mathcal{I}_{m+1,m+1}$. The matrix $\mathcal{I}$ becomes,

$$\mathcal{I} = -\frac{\omega_{pe}^2}{c^2} \begin{pmatrix} i \frac{2\sqrt{\pi}}{|k'_{\parallel m}|} \left(\omega - \hat{\omega}_{\star e}\left(1 + \frac{1}{2}\eta_e\right)\right) & 0 \\ 0 & i \frac{2\sqrt{\pi}}{|k'_{\parallel m+1}|} \left(\omega - \hat{\omega}_{\star e}\left(1 + \frac{1}{2}\eta_e\right)\right) \end{pmatrix} \tag{D17}$$

The non-diagonal terms are found to be equal to zero. This means that coupling of the modes is not achieved and the dispersion relation reduces to the one found in the previous

sections. From this equation

$$\left(\Delta'_m + \frac{\Gamma}{|k'_{\|m}|}\right)\left(\Delta'_{m+1} + \frac{\Gamma}{|k'_{\|m+1}|}\right) = 0 \tag{D18}$$

where Γ reads

$$\Gamma = i2\sqrt{\pi}\left[\omega - \hat{\omega}_{\star e}\left(1 + \frac{1}{2}\eta_e\right)\right] \tag{D19}$$

The solution is unchanged compared to the classical solution presented in the previous section. This further indicates no effect for curvature of the field on the stability of the tearing mode in the absence of particle trapping.

Appendix E: Magnetic Hamiltonian for deeply trapped particles

Without any loss of generality, the Hamiltonian can be decomposed into an equilibrium component and one leading to the magnetically trapped particles, characterized by banana orbits when projected onto the poloidal cross section, namely

$$\mathcal{H} = \mathcal{H}_{eq} + \delta\mathcal{H}_{A_\|} \tag{E1}$$

where

$$\mathcal{H}_{eq} = \frac{1}{2}mv_\|^2 + \mu B_0 \varepsilon\cos\theta \tag{E2}$$

$$\delta\mathcal{H}_{A_\|} = -ev_\|\delta A_\| \tag{E3}$$

The parallel component of the perturbed vector potential is written as a helical perturbation in real space

$$\delta A_\| = A_\|\cos\left(m\theta - n\varphi - \omega t\right) \tag{E4}$$

where $A_\|$ is the amplitude of the perturbation. However, the perturbations introduced here exist in real space and unfortunately do not have the same expression in the space of canonically conjugated variables that are suitable for the description of particle trajectories. Therefore, the hamiltonian needs to be written in terms of the action-angle variables of the deeply trapped particles. For this purpose we use the relations (derive these relations in appendix)

$$\theta = \theta_0\cos\alpha_2 \tag{E5}$$

$$\varphi = \alpha_3 + q\theta_0\cos\alpha_2 \tag{E6}$$

Note that the previous expressions, although strictly speaking valid for deeply trapped particles, can be applied for poloidal angles up to $\theta_0 \approx \pi/2$ and therefore apply also for trapped particles (not barely particles though). Moreover, the parallel velocity can be expressed in terms of the angle α_2,

$$v_\| = -\frac{\theta_0\omega_2}{J}\sin\alpha_2 \tag{E7}$$

or equivalently

$$v_\| = -\frac{\theta_0\omega_2}{i2J}\left(\mathrm{e}^{i\alpha_2} - \mathrm{e}^{-i\alpha_2}\right) \tag{E8}$$

where $J = \frac{\mathbf{B}_{\mathrm{eq}}\cdot\nabla\theta}{B_{\mathrm{eq}}}$ is the projection of the unit vector along the magnetic field line onto the poloidal direction. The parallel component of the vector potential is re-written as

$$\delta A_\| = \frac{A_\|}{2}\left(\mathrm{e}^{i(m\theta - n\varphi - \omega t)} + \mathrm{e}^{-i(m\theta - n\varphi - \omega t)}\right) \tag{E9}$$

Introducing the expressions E5 and E6 that provide θ and φ as functions of α_2 and α_3 we obtain

$$\delta A_\| = \frac{A_\|}{2}\left(\mathrm{e}^{i(m\theta - n\varphi - \omega t)} + \mathrm{e}^{-i(m\theta - n\varphi - \omega t)}\right) \tag{E10}$$

where $J_p\left(x\right)$ is the Bessel function of the first kind of order p. We have used the following properties of the Bessel functions

$$\mathrm{e}^{ix\cos\alpha_2} = \sum_{p=-\infty}^{+\infty} i^p J_p\left(x\right)\,\mathrm{e}^{ip\alpha_2} \tag{E11}$$

and

$$J_p\left(-x\right) = \left(-1\right)^p J_p\left(x\right) \tag{E12}$$

Now we have to multiply this expression by the parallel velocity expressed in terms of α_2 to obtain

$$\mathcal{H}_{A_\|} = \frac{e\theta_0\omega_2 A_\|}{i4J}\sum_{p=-\infty}^{+\infty}\left(-1\right)^p J_{2p}\left(\left(m - nq\right)\theta_0\right) \times\left(\mathrm{e}^{i(2p+1)\alpha_2} - \mathrm{e}^{i(2p-1)\alpha_2}\right)\left(\mathrm{e}^{i(n_3\alpha_3+\omega t)} + \mathrm{e}^{-i(n_3\alpha_3+\omega t)}\right) \tag{E13}$$

The shift in p can be transferred from the complex exponential to the Bessel function to give

$$\mathcal{H}_{A_\|} = \frac{e\theta_0\omega_2 A_\|}{i4J}\sum_{n_2\,\mathrm{odd}}\left(-1\right)^{\frac{n_2-1}{2}}\left[J_{n_2-1}\left(\left(m + nq\right)\theta_0\right) + J_{n_2+1}\left(\left(m + nq\right)\theta_0\right)\right]\mathrm{e}^{in_2\alpha_2}\left(\mathrm{e}^{i(n_3\alpha_3+\omega t)} + \mathrm{e}^{-i(n_3\alpha_3+\omega t)}\right) \tag{E14}$$

Now we can use the property

$$J_{p+1}\left(x\right) + J_{p-1}\left(x\right) = \frac{2p}{x}J_p\left(x\right) \tag{E15}$$

which results in the expression

$$\mathcal{H}_{A_\|} = \frac{e\theta_0\omega_2 A_\|}{i2J}\sum_{n_2\,\mathrm{odd}}\left(-1\right)^{\frac{n_2-1}{2}} n_2\frac{J_{n_2}\left(\left(m + nq\right)\theta_0\right)}{\left(m + nq\right)\theta_0} \times\mathrm{e}^{in_2\alpha_2}\left(\mathrm{e}^{i(n_3\alpha_3+\omega t)} + \mathrm{e}^{-i(n_3\alpha_3+\omega t)}\right) \tag{E16}$$

Finally, the n_2, n_3, ω component of the perturbed hamiltonian is found to be

$$\delta\mathcal{H}_{A_\parallel,n_2,n_3,\omega} = \begin{cases} \frac{e\theta_0\omega_2}{i2J}\,(-1)^{\frac{n_2-1}{2}}\; n_2 \frac{J_{n_2}(\ (m+nq)\theta_0)}{(m+nq)\theta_0} A_\parallel & \text{if } \mathrm{n_2}\,\text{is odd} \\ 0 & \text{if } \mathrm{n_2}\,\text{is even} \end{cases} \tag{E17}$$

which reduces to $\delta\mathcal{H}_{A_\parallel,n_2=0,n_3,\omega} = 0$.

REFERENCES

[1] Harold P Furth, John Killeen, and Marshall N Rosenbluth. Finite-resistivity instabilities of a sheet pinch. *The Physics of Fluids*, 6(4):459–484, 1963.

[2] J. Daintith and E. Wright. *A Dictionary of Computing*. Oxford Paperback Reference. OUP Oxford, 2008.

[3] John Wesson. *Tokamaks*, volume 149. Oxford university press, 2011.

[4] Alexandre Poye. *Dynamique des ilots magnétiques en présence de feuille de courant et en milieu turbulent*. PhD thesis, 2012. Thèse de doctorat dirigée par Mohamed-Benkadda, Mohamed Sadruddin Astrophysique et Cosmologie Aix-Marseille 2012.

[5] Milton Abramowitz, Irene A Stegun, et al. *Handbook of mathematical functions with formulas, graphs, and mathematical tables*, volume 9. Dover, New York, 1972.

[6] AG Peeters, Y Camenen, F James Casson, WA Hornsby, AP Snodin, D Strintzi, and Gabor Szepesi. The nonlinear gyro-kinetic flux tube code gkw. *Computer Physics Communications*, 180(12):2650–2672, 2009.

[7] W. A. Hornsby, P. Migliano, R. Buchholz, L. Kroenert, A. Weikl, A. G. Peeters, D. Zarzoso, E. Poli, and F. J. Casson. The linear tearing instability in three dimensional, toroidal gyro-kinetic simulations. *Physics of Plasmas*, 22(2):022118, 2015.

[8] A. K. Sundaram and A. Sen. Gyrokinetic analysis of tearing instabilities in a collisionless plasma. *Physics of Plasmas*, 18(3):032112, 2011.

[9] S Nasr, AI Smolyakov, P Migliano, D Zarzoso, X Garbet, and S Benkadda. Interchange destabilization of collisionless tearing modes by temperature gradient. *Physics of Plasmas*, 25(7):074503, 2018.

[10] Masahiro Hoshino. The electrostatic effect for the collisionless tearing mode. *Journal of Geophysical Research: Space Physics*, 92(A7):7368–7380, 1987.

[11] A. H. Glasser, J. M. Greene, and J. L. Johnson. Resistive instabilities in general toroidal plasma configurations. *The Physics of Fluids*, 18(7):875–888, 1975.